AGU100 ADVANCING EARTH AND SPACE SCIENCE

Tectonics

RESEARCH ARTICLE
10.1029/2017TC004901

Southwest Pacific Absolute Plate Kinematic Reconstruction Reveals Major Cenozoic Tonga-Kermadec Slab Dragging

Suzanna H. A. van de Lagemaat[1], Douwe J. J. van Hinsbergen[1], Lydian M. Boschman[1], Peter J. J. Kamp[2], and Wim Spakman[1,3]

[1]Department of Earth Sciences, Utrecht University, Utrecht, Netherlands, [2]School of Science, University of Waikato, Hamilton, New Zealand, [3]Center for Earth Evolution and Dynamics (CEED), University of Oslo, Oslo, Norway

Key Points:
- Tonga-Kermadec subduction zone is likely only ~30 Ma old
- Northward Australian absolute plate motion is illustrated by 1,500 km offset between South Loyalty Basin slab and New Caledonian suture
- Tonga-Kermadec slab was dragged 1,200 km northward through the mantle, alongside eastward rollback

Supporting Information:
- Supporting Information S1
- Data Set S1
- Data Set S2

Correspondence to:
S. H. A. van de Lagemaat and D. J. J. van Hinsbergen,
suzannavdl@gmail.com;
d.j.j.vanhinsbergen@uu.nl

Citation:
van de Lagemaat, S. H. A., van Hinsbergen, D. J. J., Boschman, L. M., Kamp, P. J. J., & Spakman, W. (2018). Southwest Pacific absolute plate kinematic reconstruction reveals major Cenozoic Tonga-Kermadec slab dragging. *Tectonics*, *37*, 2647–2674. https://doi.org/10.1029/2017TC004901

Received 21 NOV 2017
Accepted 12 JUL 2018
Accepted article online 26 JUL 2018
Published online 18 AUG 2018

©2018. The Authors.
This is an open access article under the terms of the Creative Commons Attribution-NonCommercial-NoDerivs License, which permits use and distribution in any medium, provided the original work is properly cited, the use is non-commercial and no modifications or adaptations are made.

Abstract Tectonic plates subducting at trenches having strikes oblique to the absolute subducting plate motion undergo trench-parallel slab motion through the mantle, recently defined as a form of "slab dragging." We investigate here long-term slab-dragging components of the Tonga-Kermadec subduction system driven by absolute Pacific plate motion. To this end we develop a kinematic restoration of Tonga-Kermadec Trench motion placed in a mantle reference frame and compare it to tomographically imaged slabs in the mantle. Estimating Tonga-Kermadec subduction initiation is challenging because another (New Caledonia) subduction zone existed during the Paleogene between the Australia and Pacific plates. We test partitioning of plate convergence across the Paleogene New Caledonia and Tonga-Kermadec subduction zones against resulting mantle structure and show that most, if not all, Tonga-Kermadec subduction occurred after ca. 30 Ma. Since then, Tonga-Kermadec subduction has accommodated 1,700 to 3,500 km of subduction along the southern and northern ends of the trench, respectively. When placed in a mantle reference frame, the predominantly westward directed subduction evolved while the Tonga-Kermadec Trench underwent ~1,200 km of northward absolute motion. We infer that the entire Tonga-Kermadec slab was laterally transported through the mantle over 1,200 km. Such slab dragging by the Pacific plate may explain observed deep-slab deformation and may also have significant effects on surface tectonics, both resulting from the resistance to slab dragging by the viscous mantle.

Plain Language Summary In studying subduction zones, where one plate dives below another back into the mantle, we tend to focus on the relative motion between the two plates, normally by assuming that the upper plate is fixed relative to the underlying mantle. Plate reconstructions in an "absolute" mantle frame of reference show, however, that trenches often migrate parallel to their trend relative to the mantle. In this paper, we study the southwestern Pacific Tonga-Kermadec Trench and demonstrate (1) that it is likely much younger than often assumed, and accommodated most if not all of its subduction after ~30 million years ago and (2) that even in this short time period, it moved as much as 1,200 km northward relative to the mantle, parallel to its strike. By comparing this history with the subducted plate that is seismically imaged in the mantle, we show that the subducted Pacific lithosphere underwent major northward slab dragging through the mantle. This dragging explains enigmatic deep earthquakes and seismological observations of mantle structure. Realizing the role of slab dragging may provide novel constraints for deep-time geological reconstructions as well as natural hazards assessment.

1. Introduction

By its definition, lithosphere subduction operates by a trench-normal influx of lithosphere into the mantle. Deep subduction is considered to be primarily driven by slab pull (Conrad & Lithgow-Bertelloni, 2002; Turcotte & Schubert, 2002), which may tend to force the trench to be normal to subduction. Perhaps for these reasons the investigation of subduction kinematics and dynamics is frequently focused on slab motion orthogonal to trenches (e.g., Heuret & Lallemand, 2005; Schellart et al., 2008). Tectonic plates, however, often subduct along trenches with varying orientations relative to their subducting plate motion in an absolute plate motion frame of reference (Goes et al., 2011; Philippon & Corti, 2016). The gravitational pull acting on the subducting parts of a plate contributes to the overall plate motion, but as a rheologically strong plate undergoes one average motion about an Euler pole at a particular time, by implication slabs may undergo trench-parallel motions through the mantle. The Pacific plate, being the largest plate on Earth, serves as a prime example of a

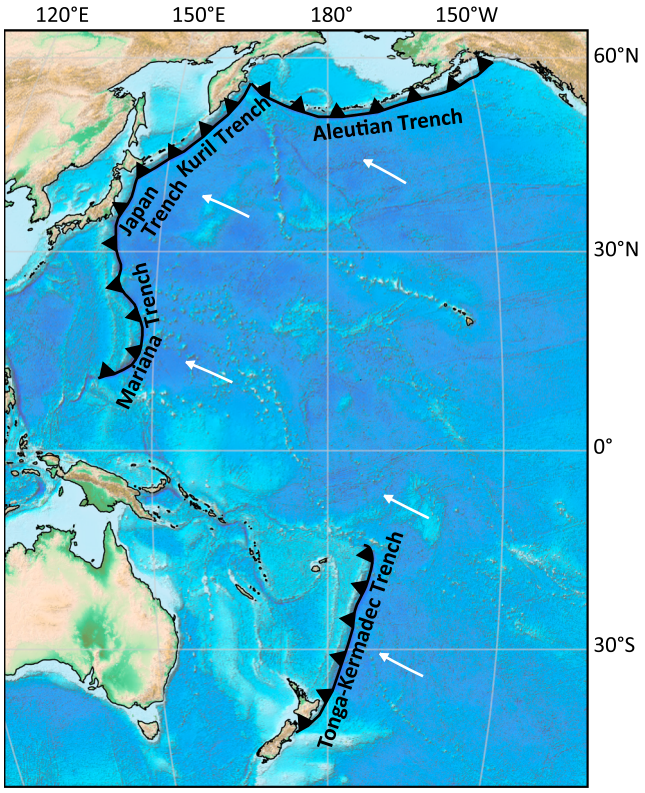

Figure 1. Present-day trenches in the western Pacific realm. White arrows indicate absolute Pacific plate motion for the last 10 Myr (based on our model, see Table 3 and the supporting information). The varying degrees of obliquity at Pacific subduction zones requires that during the last 10 Myr, the slabs subducting at these trenches must have undergone a component of trench-parallel absolute motion defined as "slab dragging." Background map from Amante and Eakins (2009).

plate having subducting slabs of varying orientations at present. The Tonga-Kermadec and Mariana trenches roughly strike N-S, Japan and the Kuril trenches strike NE-SW and the Aleutian Trench strikes roughly E-W (Figure 1). When placed in a mantle reference frame (e.g., the moving hot spot reference frames of O'Neill et al., 2005, Torsvik et al., 2008, or Doubrovine et al., 2012), the Pacific plate has an overall NW-ward absolute plate motion, from which it follows that slabs of the Pacific plate must undergo trench-parallel motion where a trench is oriented oblique to the local direction of absolute Pacific plate motion. This trench-parallel slab motion is a form of "slab dragging" (Chertova et al., 2014) and comprises in general any lateral slab transport through the mantle that results from the absolute surface motion of the subducting plate (Spakman et al., 2018). Slab dragging also includes any trench-normal slab advance that is caused by the subducting plate motion and which acts against slab rollback, as has been observed in laboratory experiments (Schellart, 2005). Slab dragging includes the exceptional cases where entire subduction systems are being dragging laterally through the mantle in directions independent of trench orientation (Spakman et al., 2018). Previous examples of slab dragging are the northward trench-parallel dragging of the Burma slab as part of the India plate (Le Dain et al., 1984), the NNE-ward transport of the entire Banda slab by the Australian plate (Spakman & Hall, 2010), slab "stumps" under western North-America that are laterally dragged by the Pacific plate (Furlong & Govers, 1999; Pikser et al., 2012; Wang et al., 2013), and the NNE-ward dragging of the entire Gibraltar slab by African plate motion (Spakman et al., 2018). The last example, which is particularly pertinent here, is that of Giardini and Woodhouse (1986), who attributed the strong horizontal deformation of the Tonga-Kermadec slab to horizontal shear interaction with the mantle. They proposed that the shear interaction is possibly induced by roughly northward trench-parallel transport of the slab through the mantle.

By reconstruction of the SW Pacific tectonic evolution during the Cenozoic, we here analyze the extent to which the Tonga-Kermadec subduction zone in the southwest Pacific may have been dragged northward through the mantle. At present, the Tonga-Kermadec subduction zone extends for approximately 2,700 km from the east coast of North Island, New Zealand, to south of Samoa (Figure 2). This subduction zone accommodates convergence between the Pacific and Australian plates and is the location of the highest rates of Pacific plate subduction and overriding plate extension (Bevis et al., 1995). The Tonga-Kermadec subduction zone is associated with a long, westward dipping subducted slab located below the present-day SW Pacific region that is well imaged by seismic tomography (Bijwaard et al., 1998; Fukao et al., 2001; Fukao & Obayashi, 2013; Gorbatov & Kennett, 2003; Hall & Spakman, 2002, 2004; Schellart et al., 2009; Schellart & Spakman, 2012; Van der Meer et al., 2018; Van der Hilst, 1995). This slab has penetrated the lower mantle along most of its length and reaches depths of at least ~1,200 km. In the northern part of the Tonga-Kermadec subduction system and at the 660-km discontinuity between the upper and lower mantle, the slab is flat lying to shallow dipping, whereas in the south, it is steeply dipping into the lower mantle (Figure 3).

In the context of relative Australian-Pacific plate convergence, the dynamics and structure of the Tonga-Kermadec subduction zone and its slab are well known, whereas the motion of the system in an absolute plate motion frame of reference remains less extensively explored. The moving hot spot reference frame (e.g., Doubrovine et al., 2012; O'Neill et al., 2005; Torsvik et al., 2008) suggests that the Australia and Pacific plates have shared a component of rapid northward absolute plate motion of up to ~7 cm/year during the Cenozoic. This shared absolute plate motion component is invisible in a relative plate motion reconstruction of Tonga-Kermadec subduction but must strongly influence the motion of the Tonga-Kermadec Trench relative to the mantle. Plate tectonic indications that such motion may actually have occurred are suggested by previous reconstructions presented by Sdrolias and Müller (2006), or Faccenna et al. (2012), for example,

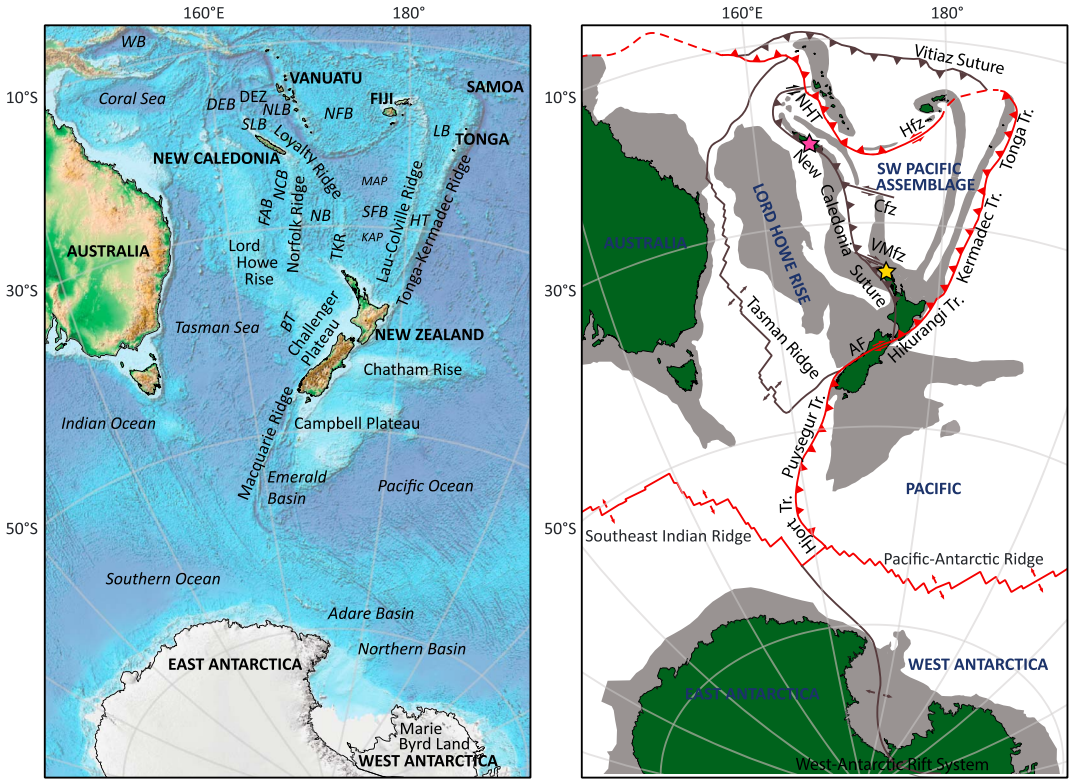

Figure 2. Topography and bathymetry (left) and tectonic map (right) of the SW Pacific. Tectonic map is based on our model (see Table 3 and the supporting information): continents in green, submerged continental fragments and volcanic arcs in gray. Present-day plate boundaries in red, former plate boundaries in dark gray. Pink and yellow stars are locations of New Caledonia and Northland ophiolites, respectively. (Former) plate names in dark blue. SW Pacific assemblage consists of multiple smaller plates. BT = Bellona Trough; DEB = D'Entrecasteaux Basin; DEZ = D'Entrecasteaux Zone; FAB = Fairway-Aotea Basin; HT = Havre Trough; KAP = Kupe Abyssal Plain; MAP = Minerva Abyssal Plain = NB, Norfolk Basin; NCB = New Caledonia Basin; NFB = North Fiji Basin; NLB = North Loyalty Basin; LB = Lau Basin; SFB = South Fiji Basin; SLB = South Loyalty Basin; WB = Woodlark Basin; NHT = New Hebdrides Trench; Cfz = Cook fracture zone; Hfz = Hunter fracture zone; VMfz = Vening Meinesz fracture zone; Tr = Trench.

although left uninterpreted in terms of subduction zone dynamics. Here we investigate in particular the scale at which slab dragging may have affected the Tonga-Kermadec subduction zone and whether such influence may be evident from the position of the associated subducted slabs.

To this end, it is first necessary to estimate when subduction along the Tonga-Kermadec Trench started. Despite being one of the most spectacular subduction zones on Earth today, the age of its initiation proves to be difficult to assess and different ages have been suggested in the past. A widely held view is that subduction started around 45–50 Ma (e.g., Matthews et al., 2015), correlating it to an Eocene global-scale plate reorganization (e.g., Whittaker et al., 2007). This age corresponds to interpretations made by Bloomer et al. (1995) based on $^{40}Ar/^{39}Ar$ dated samples of a quartz gabbro and a tholeiitic basalt from the island of 'Eua, Tonga (46.6 and 46.1 Ma, respectively; Ewart et al., 1977). However, other reconstructions have suggested ages of subduction initiation ranging from 90 Ma or even earlier (Schellart et al., 2006), to as young as 27 Ma (Yan & Kroenke, 1993).

One of the main reasons for uncertainty around the age of the Tonga-Kermadec subduction system is that it is not possible to make a Cenozoic closed plate circuit involving the Tonga-Kermadec subduction zone as the area between eastern Australia and the Pacific Ocean hosted two Cenozoic subduction systems: the modern Tonga-Kermadec system and a former New Caledonia subduction system that led to Late Cretaceous-Paleogene formation and Early Miocene emplacement of an ophiolite belt on New Caledonia (Figures 2 and 4; e.g., Cluzel, Jourdan, et al., 2012; Schellart et al., 2009). The area between these two trenches (here referred to as the SW Pacific assemblage) underwent a complex Cenozoic history of back-arc spreading.

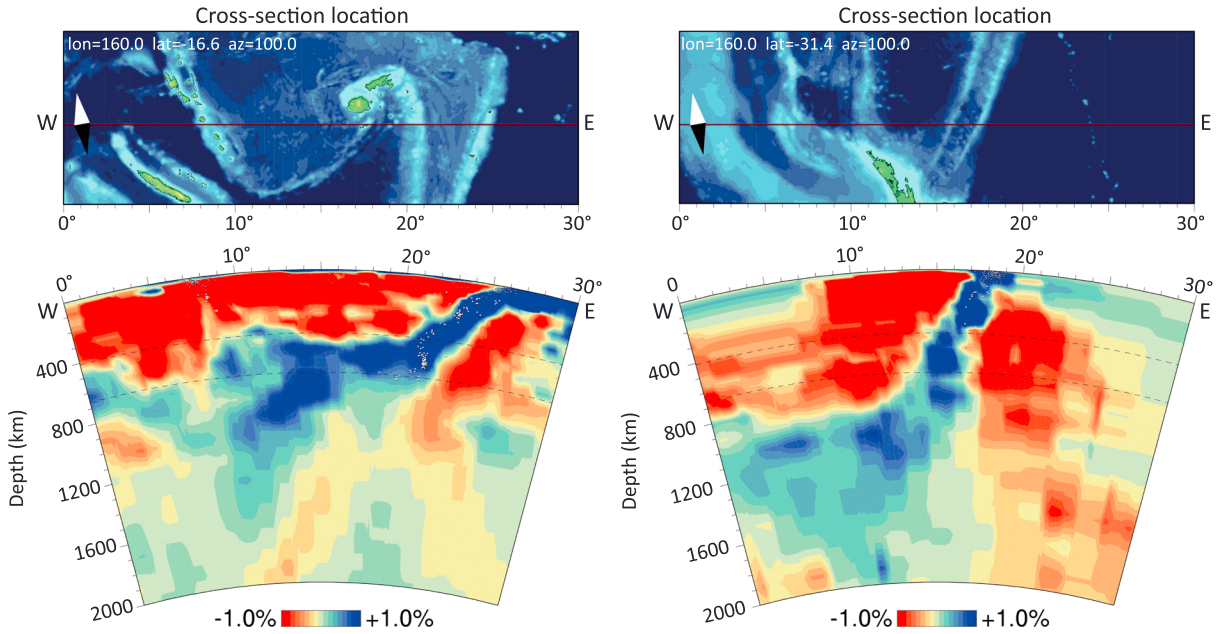

Figure 3. W-E tomographic cross sections of the Tonga-Kermadec slab at the northern (left) and southern (right) ends of the trench, based on the UU-P07 tomographic model (Amaru, 2007). In the north, a significant portion of the slab is flat lying before it continues into the upper mantle, whereas in the south the slab penetrates straight into the upper mantle.

While it is possible to reconstruct how much net convergence occurred and how much additional subduction must have occurred to accommodate the opening of the well-known extensional back-arc basins between the Tonga-Kermadec Trench and Australia, it is less straightforward to reconstruct how and when this convergence was distributed between the New Caledonia and Tonga-Kermadec subduction zones. Prior tectonic reconstructions of the SW Pacific assemblage have included a New Caledonia subduction zone (e.g., Matthews et al., 2015; Schellart et al., 2006; Yan & Kroenke, 1993), but how Pacific-Australia convergence was distributed between the two subduction zones has never been addressed and what it means for the age of the Tonga-Kermadec subduction system.

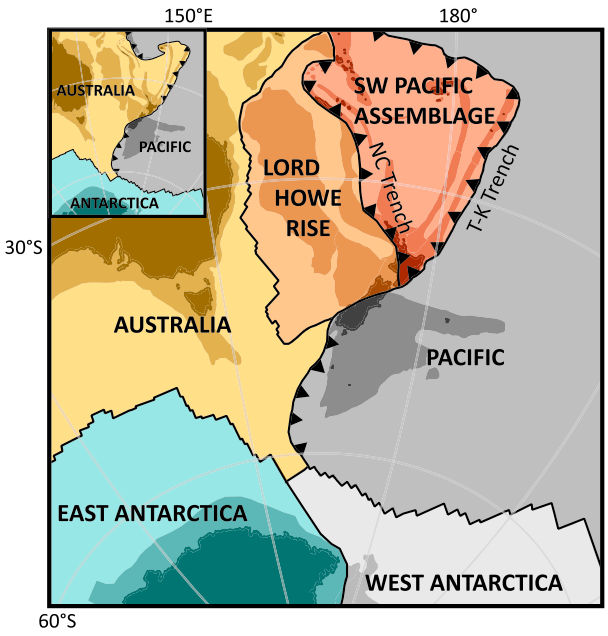

Figure 4. Plate tectonic setting of the SW Pacific region during the Late Cretaceous to Cenozoic (based on our model, see Table 3 and the supporting information). Inset: Present day plate configuration. The SW Pacific assemblage is surrounded by subduction zones that may have been active contemporaneously, which makes it difficult to make a definitive closed plate circuit for the Paleogene.

Our approach to resolving how subduction at the Tonga-Kermadec Trench responded to rapid absolute plate motion with a strong trench-parallel component is as follows: (i) development of a plate kinematic reconstruction of the SW Pacific region cast within the Australia-Pacific plate circuit; (ii) testing partitioning of plate convergence across the New Caledonia and Tonga-Kermadec subduction zones against resulting mantle structure inferred from tomography; (iii) making inferences about the possible age range of Tonga-Kermadec subduction initiation and its subduction rate through time; and (iv) assessing how the Tonga-Kermadec Trench and slab responded to absolute plate motions of the Pacific and Australian plates.

2. Seismic Tomographic Constraints on SW Pacific Mantle Structure

Seismic tomography has revealed several anomalies in the SW Pacific region that are interpreted to reflect subducted slabs. Here we use tomographic model UU-P07 (Amaru, 2007) of which slab interpretations for this region were made by Hall and Spakman (2002), Schellart et al. (2009), Schellart and Spakman (2012, 2015), and Van der Meer

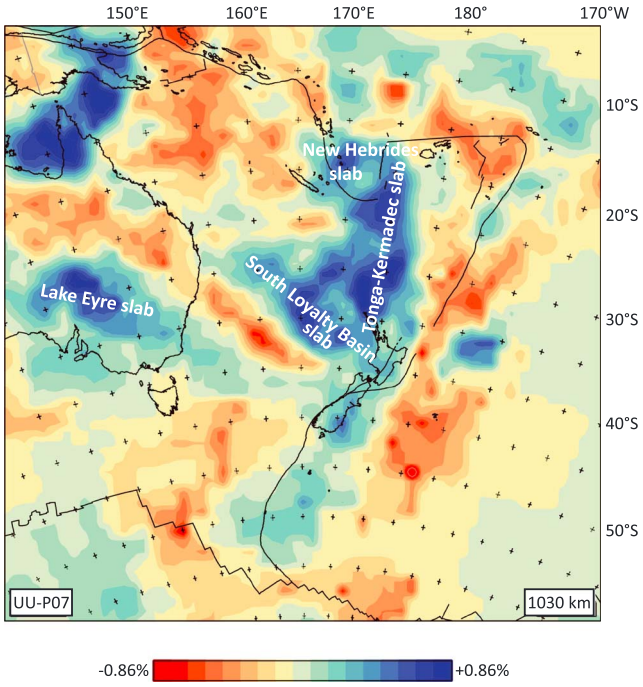

Figure 5. Tomographic image from the southwest Pacific region at a depth of 1,030 km, revealing the Tonga-Kermadec, South Loyalty Basin, Lake Eyre, and New Hebrides slabs, based on the UU-P07 tomographic model (Amaru, 2007). See section 2 for description of the contour parameters in the legend scale bar.

et al. (2018; Figure 5). In Figures 5 and 6 the percentage limits defined in the legends and applied in the map plots of the *P* wave velocity anomalies vary with depth. These limits are depth dependent following the relationship between *P* wave velocity and temperature as a function of depth, as established by Goes et al. (2004). The scaling is such that the contour limits always correspond to an estimated temperature anomaly of −250 K (for the positive limit) and +250 K (for the negative limit). Thus, implicitly, the tomography map-view images also provide an estimate of the mantle temperature anomaly. This also emphasizes that while *P* wave velocity percentages in the lower mantle are generally small (<1%), the corresponding temperature anomaly can be on the order of 10% of the ambient lower mantle temperature.

The most prominent anomaly in the SW Pacific is related to the Tonga-Kermadec slab (Hall & Spakman, 2002; Van der Hilst, 1995). The slab is west dipping, and located west of the present-day subduction zone, up to a depth of ~1,200 km along the whole length of the trench (Figure 6; Schellart & Spakman, 2012). In the south, the slab penetrates almost straight through the 660-km discontinuity into the lower mantle, whereas in the north, a significant portion of the slab lies horizontally over the 660-km discontinuity before it dips into the lower mantle at its western end (Figure 3). This leads to a N-S striking anomaly below the 660-km discontinuity and a clockwise rotation of the anomaly at successively shallower depths to its present-day NNE-SSW configuration.

The anomaly considered to be related to the New Caledonia subduction zone was first identified by Schellart et al. (2009) and is referred to as the South Loyalty slab (Cluzel et al., 2001; Schellart, 2007; Schellart et al., 2006, 2009). It is located ~1,500 km south of New Caledonia, currently below the Tasman Sea, in the upper part of the lower mantle at ~950 to 1,350 km depth and is best resolved at ~1,000–1,200 km (Figure 5). The slab trends NW-SE and is flat lying with a lateral extent of ~2,200 by 600–900 km (Figures 5 and 7; Schellart et al., 2009). In the southeast, the South Loyalty slab is difficult to distinguish from the southern end of the Tonga-Kermadec slab, as the bases of both slabs are located at approximately the same depth (Figure 5).

A third anomaly is located in the SW Pacific, related to ongoing northeast dipping subduction at the New Hebrides subduction zone (Figure 5). This slab is well imaged and reaches the base of the upper mantle (Fukao et al., 2001; Fukao & Obayashi, 2013; Hall & Spakman, 2002, 2004; Obayashi et al., 2013; Schellart & Spakman, 2012; Wu et al., 2016).

A fourth anomaly, not located in the SW Pacific, that is of interest to this study is located below the Lake Eyre region in Australia and is interpreted as an ENE-WSW trending slab that subducted northwards at the New Guinea-Pocklington trough (Schellart & Spakman, 2015). The slab is currently located in the upper part of the lower mantle at 800–1,200 km depth (Figure 5). Timing of slab break-off is interpreted from the final obduction of the ophiolite on New Guinea and in the Pocklington area at about 50 Ma (Schellart & Spakman, 2015).

Interestingly, the emplaced ophiolites associated with the end of subduction at the New Caledonia and Papua New Guinea subduction zones are presently located ~1,500 and ~2,800 km north of the New Caledonia and Lake Eyre slabs, respectively. The Australian plate overrode these detached slabs evidencing its northward absolute plate motion (Schellart & Spakman, 2015).

3. Australia-Pacific Plate Circuits

A relative plate circuit using a kinematic reconstruction needs to be constructed to study the convergence history between the Pacific and Australian plates. Such a circuit includes five major (former) tectonic plates: Lord Howe Rise (including the northern part of the New Zealand continent, hereafter abbreviated to LHR),

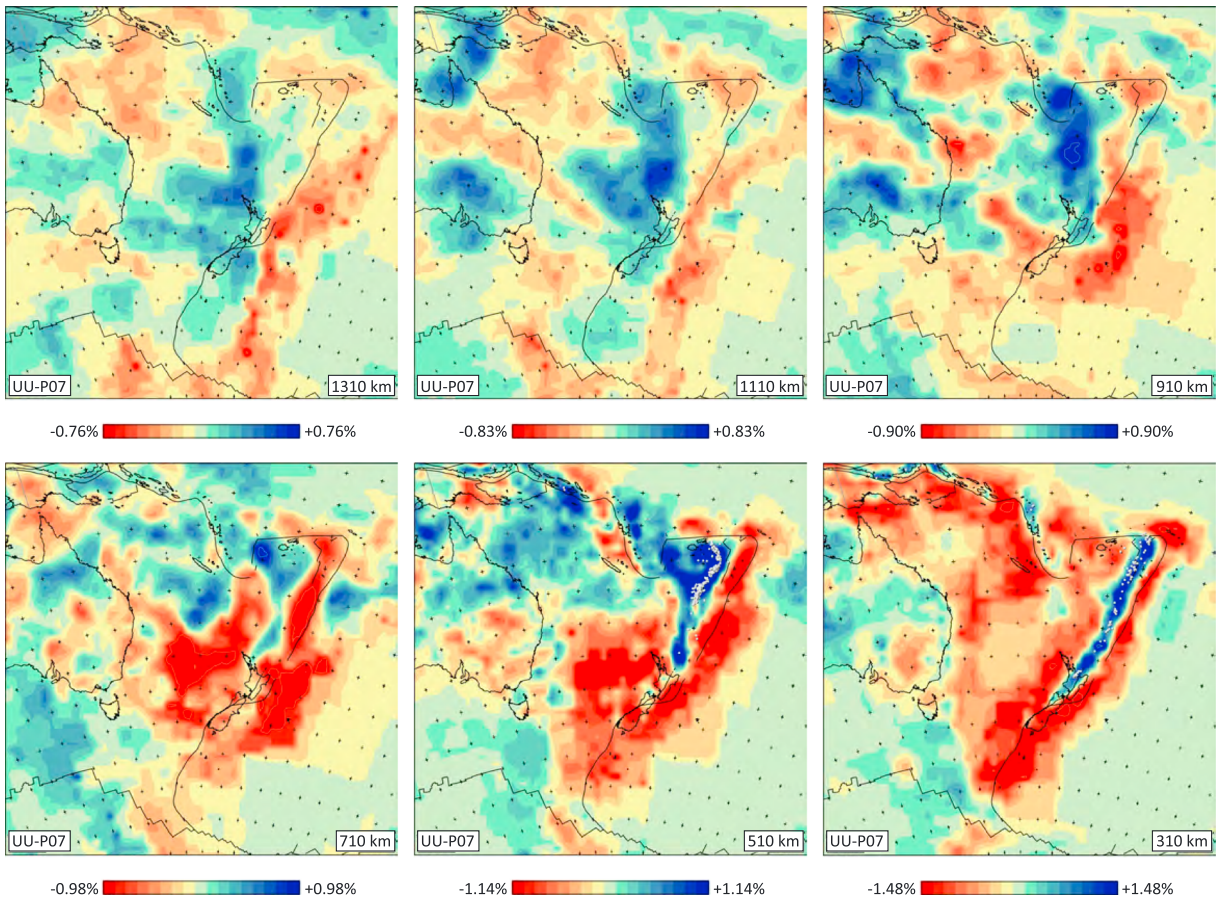

Figure 6. Seismic tomographic images of the SW Pacific regions at successive shallower depths, based on the UU-P07 tomographic model (Amaru, 2007). See section 2 for description of the contour parameters in the legend scale bars. These images illustrate that the entire Tonga-Kermadec slab is located west of the present-day trench along the entire length of the trench, and no southward deflection relative to the present-day trench is visible. The upper mantle portion of the slab is also located west of the present-day trench.

Australia (AUS), East Antarctica (eANT), West Antarctica (wANT), and Pacific (PAC; Figure 4). Motion at the plate boundaries between AUS-eANT, AUS-LHR, and PAC-wANT is constrained by marine magnetic anomalies and transform faults/fracture zones of oceanic crust produced by former or active ridges (e.g., Croon et al., 2008; Gaina et al., 1998; Tikku & Cande, 1999, 2000; Whittaker et al., 2007, 2013; Wright et al., 2015, 2016). The boundaries between LHR and PAC in New Zealand (e.g., Alpine Fault) and between eANT and wANT (the West Antarctic Rift system) are, however, less well defined (Figure 2). Motion along these plate boundaries can be partly constrained by magnetic anomalies occurring in adjacent oceanic lithosphere, but typically only for brief intervals (Granot et al., 2013a, 2013b; Keller, 2004).

Motion between eANT and wANT is constrained between ~40 and 26 Ma by marine magnetic anomalies in the Adare Basin and adjacent Northern Basin (Cande et al., 2000; Cande & Stock, 2004; Granot et al., 2013a). However, it has been tentatively suggested that extension in the Adare Basin started around 60 Ma (Cande & Stock, 2004) and, additionally, apatite fission track thermochronology suggests that the West Antarctic Rift system was actively extending between ~100 and 60 Ma (Spiegel et al., 2016). Consequently, marine magnetic anomalies do not provide sufficient constraints on the eANT-wANT plate boundary evolution.

Motion between LHR and PAC is constrained by marine magnetic anomalies of the Macquarie spreading center between ~40 and 24 Ma (Keller, 2004). The uncertainty ellipses of these rotation poles are relatively large as a result of the short strike-length of the anomalies mapped in Emerald Basin and southern Tasman Sea. Also, part of this original seafloor west of Macquarie Ridge has been consumed by subduction at Puysegur Trench (Keller, 2004) and hence the age structure of this former seafloor cannot be reconstructed. Post-28 Ma dextral bending of seafloor and fracture zones adjacent to the AUS-PAC plate boundary between

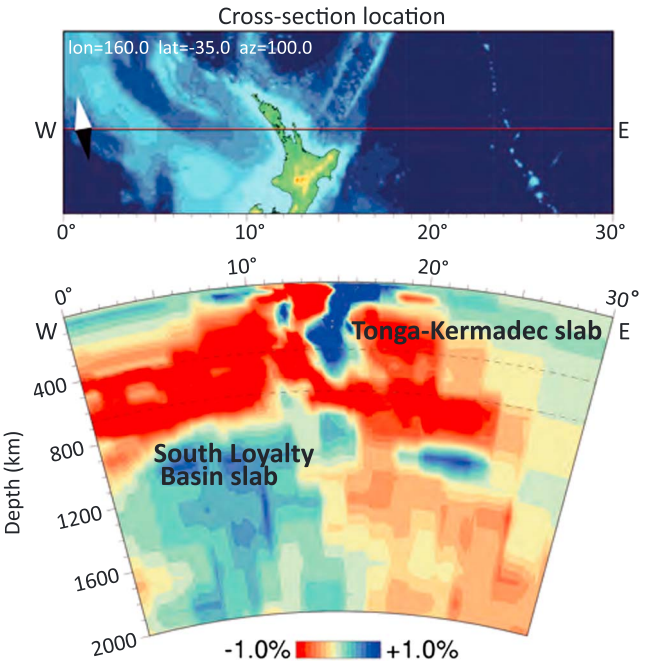

Figure 7. W-E tomographic cross section of the South Loyalty Basin slab, based on the UU-P07 tomographic model (Amaru, 2007).

Hjort and Puysegur trenches also contributes to the size of the Keller (2004) uncertainty ellipses (Hayes et al., 2009).

Because there are two poorly constrained plate boundaries in the circuit, two alternative plate motion circuits have been previously proposed (Figure 8): an Australian circuit, in which LHR is attached to PAC until 45 Ma and the eANT-wANT boundary is left unconstrained, and an Antarctic circuit, in which the LHR-PAC boundary is left unconstrained, while motion within the West Antarctic Rift system is incorporated (e.g., Doubrovine et al., 2012; Doubrovine & Tarduno, 2008a, 2008b; Matthews et al., 2015; Schellart et al., 2006; Steinberger et al., 2004).

Matthews et al. (2015) recently provided an extensive review and analysis of SW Pacific plate circuits. They tested a total of six Antarctic circuit scenarios and four Australian circuit scenarios. These scenarios differ in rotation poles used for the eANT-AUS and wANT-PAC spreading ridges. In the Antarctic circuit, different eANT-wANT rotations are also tested, while in the Australian circuit PAC is attached to LHR until 45 Ma (i.e., throughout their reconstruction period). In all scenarios, AUS-LHR motion is described using the finite rotation poles provided by Gaina et al. (1998). The different scenarios are used to explore the implications of the two plate circuits for the amount and type of deformation predicted within New Zealand and in the West Antarctic Rift system, and to the north of New Zealand. Matthews et al. (2015) proposed that after 55 Ma, the Antarctic circuit, using rotation poles of Whittaker et al. (2013), Granot et al. (2013a, 2013b), and Larter et al. (2002) for AUS-eANT, wANT-eANT, and PAC-wANT motions, respectively, produces the best fit with geological observations from both New Zealand and the West Antarctic Rift system. This plate circuit has been incorporated into the global plate model of Müller et al. (2016). Additionally, in the global plate model of Müller et al. (2016), PAC-wANT motion is updated using the finite rotation poles of Wright et al. (2015, 2016).

Because the models of Matthews et al. (2015) and Müller et al. (2016) produce fits that reasonably satisfy geological constraints for both the plate boundary through New Zealand and the West Antarctic Rift system, we adopt their (Antarctic) plate circuit as a basis for our SW Pacific restoration. However, we do not directly follow the reconstruction of Müller et al. (2016) but use it as a framework. We choose to use all finite rotation poles as published in the original papers (Table 1), whereas Müller et al. (2016) used only a selection of chrons, leading to greater detail in our reconstruction. Additionally, we updated the ages of the chrons to the timescale of Ogg (2012).

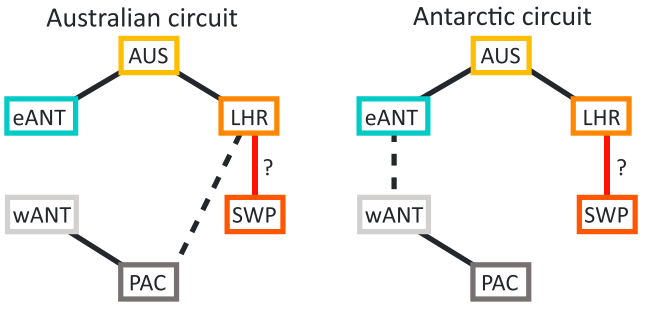

Figure 8. Australian and Antarctic plate circuits. Dashed lines indicate poorly constrained boundaries within each circuit. The plate motion chain to connect LHR and the southwest Pacific assemblage (SWP) is uncertain in both plate circuits due to the existence of the New Caledonia subduction zone in the Cenozoic.

A set of Euler poles for the 40- to 24-Ma motions on the plate boundary through New Zealand was proposed by Keller (2004) that differ in details from those of the Müller et al. (2016) plate circuit. The discrepancy may have been accommodated on the poorly constrained Bellona Trough between Challenger Plateau and Lord Howe Rise where a plate boundary may have existed (e.g., Cande & Stock, 2004; Gaina et al., 1998; Van de Beuque et al., 2003). To satisfy both the Müller et al. (2016) plate circuit and the Keller (2004) constraints, our reconstruction accommodates the difference at Bellona Trough. At 24 Ma, shortly after inception of the Alpine Fault (Kamp, 1986), the unconstrained boundary is relocated from Bellona Trough to the Alpine Fault.

4. SW Pacific Plates and Kinematics

In this section we provide a review of geological data from the SW Pacific region between LHR in the west and the Tonga-Kermadec Trench in the east. This part of the SW Pacific consists of a series of

Table 1
References for the Finite Rotation Poles Used in Our Reconstruction (Antarctic Circuit)

Plate boundary	References
Lord Howe Rise-Australia	Gaina et al., 1998; Seton et al., 2012
Australia-East Antarctica	Cande & Stock, 2004; Whittaker et al., 2013
West Antarctica-East Antarctica	Granot et al., 2013a, 2013b[a]; Matthews et al., 2015
Pacific-West Antarctica	Croon et al., 2008; Wright et al., 2015, 2016
Challenger Plateau (LHR)-Campbell Plateau (PAC)	Keller, 2004

[a]We chose to omit the finite rotation pole for chron 16y, because it leads to unrealistic back-and-forth movement within the Antarctic continent between ~40 and 34 Ma. This rotation pole is subject to a greater uncertainty due to difficulty in the identification of magnetic picks of this anomaly (explained in Granot et al., 2013a).

basins and ridges comprising oceanic, continental, and arc crust, and we will review their formation age and history. Because this area is surrounded by active and fossil subduction zones, these basins and ridges are reconstructed using a separate plate motion chain (Figure 9). To this end, we first review studies based on marine geophysical constraints on the opening history of the various extensional basins and subsequently summarize geological constraints from ophiolites in New Caledonia and in New Zealand bearing on evolution of the western subduction system. This review focuses on the basins and ridges between LHR and Tonga-Kermadec Trench. The northern part of the SW Pacific region, including the Coral Sea, d'Entrecasteaux, and Woodlark Basin provide no constraints on evolution of this trench and are not reconstructed in detail here.

4.1. Extensional Basins

4.1.1. Fairway-Aotea and New Caledonia Basins

Between LHR and Norfolk Ridge, thus west of the New Caledonia ophiolite and the inferred paleo-subduction zone that led to its obduction, lie two basins separated by the Fairway Ridge: the western Fairway Basin and the eastern New Caledonia Basin. The Fairway Basin extends southward into Aotea Basin, commonly otherwise known as the southern part of the New Caledonia Basin (Figure 2).

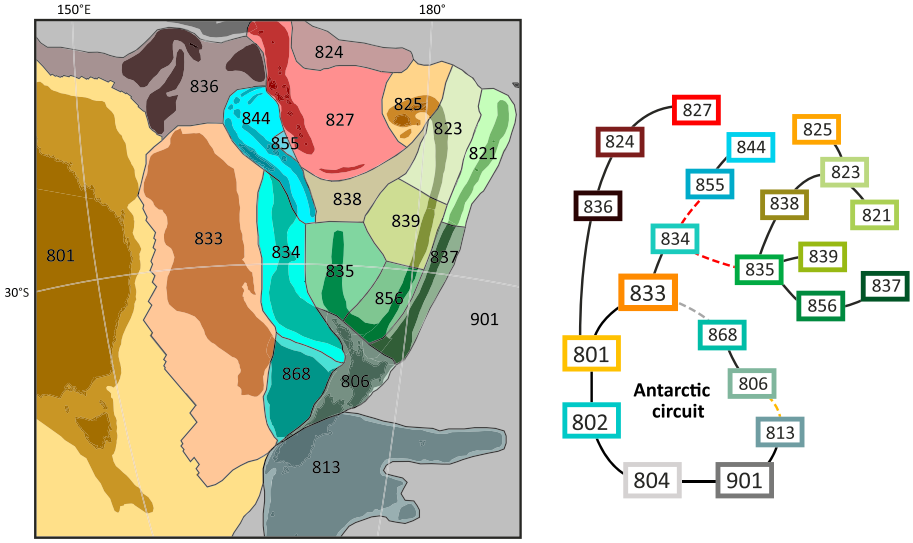

Figure 9. Tectonic units (left) and plate motion chain (right) for the SW Pacific realm. List of codes and their associated plates are found in Table 2. The unconstrained boundary between LHR and PAC is located between LHR (833) and Challenger Plateau (868) until 24 Ma (dashed gray line), and then relocated to the Alpine Fault (dashed yellow line), which marks the boundary between North New Zealand (806) and Campbell Plateau (813). Dashed red lines indicate the uncertain connection between LHR/Norfolk Ridge and the SW Pacific assemblage. These plates were separated by the New Caledonia subduction zone during its existence. LHR = Lord Howe Rise; PAC = Pacific.

Klingelhoefer et al. (2007) reported wide-angle and reflection seismic data showing that the crust of Fairway Ridge is continental and that Fairway Basin is underlain by thinned continental crust. That study also showed that New Caledonian Basin is underlain by oceanic crust in its central part. The crust in the northern part of the basin is atypical and its origin remains unknown (Klingelhoefer et al., 2007).

Owing to the difficulty of identifying the oceanic versus continental nature of crust in this part of the SW Pacific, contrasting tectonic models have been proposed. Lafoy et al. (2005) suggested that 85- to 65-Ma continental thinning in the Fairway and New Caledonia basins coincided with seafloor spreading in the southern Tasman Sea. They presume that subsequently, spreading in New Caledonia Basin occurred during the Paleocene, between ~62 and 56 Ma, concurrent with spreading in the Coral Sea Basin. Collot et al. (2009), on the other hand, suggested that extension in the Fairway and New Caledonia Basin predates Tasman Sea spreading and that these basins are early-Late Cretaceous (Cenomanian) or even older in age.

Any extension in the Fairway-Aotea and New Caledonia basins that occurred during the Late Cretaceous and later would increase the overall convergence that must have been accommodated by the subduction zones between LHR and PAC. We incorporate the scenario of Lafoy et al. (2005) and our reconstruction should thus be considered as a maximimum-convergence and subduction scenario. Using 3-D modeling of satellite gravity data, approximately 30% crustal thinning is estimated for the New Caledonia Basin (Wood & Woodward, 2002). According to Lafoy et al. (2005), however, the basin studied by Wood and Woodward (2002) structurally corresponds to the South Fairway Basin.

4.1.2. Norfolk Basin

Norfolk Basin lies between Norfolk Ridge and Three Kings Ridge (Figure 2); the age and crustal nature of which have been debated. Proposed opening ages of Norfolk Basin include Late Cretaceous (Launay et al., 1982), Eocene-Oligocene (Sdrolias et al., 2003) and Early Miocene (Mortimer et al., 1998). Deep regions within Norfolk Basin show age-bathymetry curves that would be consistent with oceanic crust that formed during the Late Oligocene to Late Miocene (Sdrolias et al., 2004). A Miocene age of spreading initiation would be consistent with a 23 ± 0.1 Ma $^{40}Ar/^{39}Ar$ age of a dredged seafloor tholeiite (Meffre et al., 2001; Bernardel et al., 2002, both cited in Sdrolias et al., 2004). Cessation of spreading in the Norfolk Basin is poorly constrained but is thought to have occurred as late as 10 Ma (Sdrolias et al., 2004).

The amount of divergence within the Norfolk Basin is estimated from displacement along the Cook and Vening Meinesz fracture zones (Figure 2). The Cook Fracture Zone is a left-lateral transform fault that offsets Three Kings Ridge from Loyalty Ridge by ~420 km (Sdrolias et al., 2004). Motion at the southern boundary of Three Kings Ridge was accommodated along the Vening Meinesz Fracture Zone. This fault offsets Three Kings Ridge dextrally from Northland Plateau and accommodated about 170 km of seafloor spreading in the southern Norfolk Basin (Herzer & Mascle, 1996). The Three Kings Ridge migrated southeastward, causing transpressive motion on the Veining Meinesz Fracture Zone (Herzer & Mascle, 1996). Motion on the Veining Meinesz Fracture Zone ended around 15 Ma, based on radiometric $^{40}Ar/^{39}Ar$ ages for two linear seamounts interpreted as mini-hot spot trails (Herzer et al., 2009; Mortimer et al., 2007). This age coincides with waning tectonism on Northland Plateau (Herzer et al., 2009, 2011).

4.1.3. North Loyalty Basin

Loyalty Ridge and North Loyalty Basin are located to the northeast of New Caledonia (Figure 2). North Loyalty Basin is a remnant of a once larger basin and is located in a triangle formed by Loyalty Ridge, New Hebrides Trench, and d'Entrecasteaux Basin (Weissel et al., 1982). Weissel et al. (1982) identified clear magnetic anomaly lineations that they tentatively correlated with chrons 23–18 (~50–40 Ma). Later reinterpretation by Sdrolias et al. (2003) reassigned these to chrons 20–16 (~44.5–36 Ma). The identified magnetic anomaly lineations were generated on the north side of a ridge. Their southern counterparts are thought to have been subducted at the New Hebrides Trench (Sdrolias et al., 2003).

4.1.4. South Fiji Basin

The South Fiji Basin extends from Fiji Islands in the north to the Northland Plateau of New Zealand in the south (Figure 2). Its eastern boundary is defined by the, now extinct, Lau-Colville volcanic arc and the western boundary is defined by the Loyalty Ridge and the Three Kings Ridge. The basin is divided into the northern South Fiji Basin or the Minerva Abyssal Plain, and the southern South Fiji Basin or Kupe Abyssal Plain (Packham & Terrill, 1975), separated by an E-W-oriented central ridge region. This ridge region is not the remnant of an actual mid-ocean ridge, but appears to be the eastward extension of the Cook Fracture Zone (Malahoff et al., 1982; Figure 2).

Anomalies 7–12 (24–31 Ma) were identified in the South Fiji Basin by Watts et al. (1977) and Malahoff et al. (1982). A complete set of anomalies from both sides of a N-S-oriented mid-ocean ridge was identified in the Minerva Abyssal Plain. A set of anomalies was identified in the Kupe Abyssal Plain by Malahoff et al. (1982), which they interpreted as younging westward. This would require that the western flank has been subducting beneath the Three Kings Ridge along a west-dipping subduction zone (Malahoff et al., 1982). Sdrolias et al. (2001), however, reinterpreted the anomalies as younging eastward, in contrast to that proposed by Malahoff et al. (1982). The absence of anomalies on the eastern half of the spreading system in the Kupe Abyssal Plain may be due to asymmetric spreading (Sdrolias et al., 2003). Sdrolias et al. (2003) computed finite rotations for both the Minerva and Kupe Abyssal Plains, based on their magnetic anomaly identifications.

More recent constraints from $^{40}Ar/^{39}Ar$ ages of abyssal tholeiites by Mortimer et al. (2007) suggest that South Fiji Basin formed during the Early Miocene, rather than during the Oligocene. The magnetic anomaly profiles are difficult to match to geomagnetic polarity reversal patterns and therefore are unsuitable to provide age constraints (Herzer et al., 2011). These authors reinterpreted the magnetic anomalies of the South Fiji Basin based on revised ages for crustal rocks from sites DSDP 205 and DSDP 285 from Mortimer et al. (2007) and concluded that the magnetic anomalies represent chrons 9 to 6B (27.4–21.9 Ma). This would mean that South Fiji Basin formed during Late Oligocene to Early Miocene, in tandem with Norfolk Basin spreading. The cessation of spreading in both basins is not well constrained but is thought to be around 15 Ma (Herzer et al., 2011; Mortimer et al., 2007).

4.1.5. Lau Basin-Havre Trough

The Lau Basin-Havre Trough is a Y-shaped active back-arc basin, immediately west of Tonga-Kermadec Trench (Figure 2). Seafloor spreading is propagating southwards and different stages of basin opening have been interpreted.

Ocean spreading currently occurs in the Lau Basin along Central and Eastern Lau spreading centers (Parson & Wright, 1996). A sequence of aeromagnetic profiles was obtained by Malahoff et al. (1994). Magnetic anomaly lineations J (C1r.1n, Jaramillo event, ~1 Ma) through 3 (4.6 Ma) were identified, indicating that seafloor spreading started around 5–7 Ma. The magnetic anomaly lineations have short lengths and spreading in the northern Lau Basin is irregular and disorganized, with multiple triple junctions and overlapping rifts (Malahoff et al., 1994). Farther south, spreading in Lau Basin more closely resembles steady state.

Extension in Havre Trough is currently in the rift phase and probably became active concurrent with extension in Lau Basin (Ruellan et al., 2003). A detailed study by Wysoczanski et al. (2010) using multibeam mapping suggested that Havre Trough is currently in an incipient phase of distributed and disorganized spreading. Because there is no magmatic spreading in Havre Trough, magnetic anomaly data do not record accretion of oceanic crust. Linear magnetic anomalies in Havre Trough, as identified by Malahoff et al. (1982), are instead interpreted as the result of pseudo-linear emplacement of magnetic sheeted dikes into arc basement rocks (Wright, 1993). Yan and Kroenke (1993) used the magnetic anomaly identifications of Malahoff et al. (1982) to compute finite rotations for Lau Basin and Havre Trough.

4.1.6. North Fiji Basin

North Fiji Basin is a Late Miocene oceanic basin currently part of the Pacific plate. It lies as overriding plate above the east-dipping New Hebrides subduction zone (Figure 2) and has a complex spreading pattern. North Fiji Basin is considered to have opened after a subduction polarity switch that followed Early Miocene (Knesel et al., 2008) or Middle Miocene (Auzende et al., 1995; Crawford et al., 2003; Petterson et al., 1997; Quarles van Ufford & Cloos, 2005) arrival of Ontong Java Plateau at Vitiaz Trench (Figure 2). New Hebrides Trench would have formed as a result of this switch and rolled back with a clockwise rotation into its current north-south orientation.

Malahoff et al. (1994) identified two spreading centers and interpreted anomalies J (C1r.1n, Jaramillo event, ~1 Ma) through 4 (1–7.6 Ma), which Yan and Kroenke (1993) used to compute finite rotation. An additional spreading center is present in northern North Fiji Basin with anomalies 2 – 3Ar (1.95–7.14 Ma) identified by Lagabrielle et al. (1996). In addition, Taylor et al. (2000) showed from paleomagnetic evidence that the Fiji Islands underwent a 135° counterclockwise rotation between 10 and 3 Ma.

4.2. Ophiolites and Volcanic Arcs

In addition to the mainly marine geophysical data listed above, key information on the location, timing, and duration of subduction between the SW Pacific region and Norfolk Ridge comes from geological constraints

provided by New Caledonian and Northland ophiolites, as well as the d'Entrecasteaux Zone, Loyalty Ridge, and Three Kings Ridge (Figure 2). Here we review key constraints on the evolution of these ophiolites and associated accretionary prisms.

4.2.1. Northland Ophiolite

The Northland Ophiolite of New Zealand, also referred to as Tangihua Complex, represents the highest structural unit of the Northland Allochthon and is composed of minor upper mantle and oceanic crustal rocks (e.g., Nicholson et al., 2007). Because of similarities in lithology and structural settings with the New Caledonia ophiolite (see below), it is thought that both ophiolites once formed at a formerly contiguous plate boundary (Malpas et al., 1992).

The age of formation of oceanic crust of the Northland ophiolite was originally thought to be of Late Cretaceous to Paleocene age (Nicholson, Picard et al., 2000). An early Paleocene age (58–62 Ma) was also suggested by Hollis and Hanson (1991) based on the presence of Paleocene radiolarian species within inter-pillow limestone. Brothers and Delaloye (1982) applied K/Ar dating to igneous rock samples from different ophiolite massifs, reporting a wide age range between 102 and 20 Ma. They therefore suggested that the Northland ophiolite complex had a long and multistage history of igneous accretion.

The older ages are confirmed by $^{40}Ar/^{39}Ar$ dating of two volcaniclastic samples that yielded ages of ca. 108 Ma (Whattam et al., 2005). Their study also suggested that at least part of the oceanic crust of the Northland Ophiolite cooled during the Oligocene. Step heating $^{40}Ar/^{39}Ar$ techniques on tholeiitic basalt samples produced ages between 25 ± 0.8 and 29.6 ± 1 Ma, and $^{206}Pb/^{238}U$ dating of zircons from a plagiogranite sample gave an age of 28.3 ± 0.2 Ma (Whattam et al., 2005). These authors thus suggested that at least two distinct groups of igneous rocks are present in the Northland Ophiolite and attributed the c. 100 Ma ages to formation of the Mt. Camel Terrane that forms the basement onto which the ophiolite was emplaced (Whattam et al., 2004, 2005, 2006).

Northland Ophiolite was emplaced during a short period during the latest Oligocene, approximately at the Oligocene-Miocene boundary. This is indicated by the Late Oligocene age of the youngest rocks in the ophiolite versus the Early Miocene age of the oldest rocks overlying the ophiolite (Ballance & Spörli, 1979). Shear sense indicators indicate that emplacement was from the northeast (Malpas et al., 1992, and references therein).

Malpas et al. (1992) reported a MORB geochemical signature in the Northland ophiolite and suggested that it was generated at a major spreading center or in a mature back-arc basin. More recent work, however, has shown that tholeiitic rocks of the ophiolite have a negative Nb anomaly and are enriched in large ion lithophile elements, which are both consistent with a suprasubduction zone signature (Nicholson, Black et al., 2000; Whattam et al., 2004, 2005).

4.2.2. New Caledonia Ophiolite

The New Caledonia archipelago consists of several islands that are part of Norfolk and Loyalty ridges (Figure 2). The main island is part of continental Norfolk Ridge. Loyalty Ridge to the north most likely represents an Eocene island arc (see below), with North Loyalty Basin interpreted as its associated back-arc basin (Cluzel, Maurizot et al., 2012).

New Caledonia exposes the Peridotite Nappe, an ophiolite complex that was emplaced onto Norfolk ridge during the Eocene. Preceding this emplacement, a north or northeast dipping subduction zone was present, as indicated by the structural history of the ophiolite and its sole (Cluzel, Maurizot et al., 2012; Quesnel et al., 2016).

The age of formation of the Peridotite Nappe is debated. Due to a complex history of the upper mantle and lower crustal section, the system became ultradepleted, making accurate dating difficult. K-Ar dating of dolerite veins, plutonic rocks (hornblendites and diorites), and of amphibole separates from a dolerite yielded an age range of 120–50 Ma (Prinzhofer, 1981, as cited in Collot et al. (1987) and Cluzel, Jourdan et al. (2012)). Lower Eocene (55–50 Ma) mafic dykes, dated by the U/Pb zircon system, crosscut the ophiolite at all levels (Cluzel et al., 2006). This indicates a minimum Late Paleocene age for formation of oceanic crust of the Peridotite Nappe. The oceanic ridge that produced the ophiolite was likely oriented E-W (in present-day coordinates), based on N-S-oriented stretching lineations measured in the mantle section of the Peridotite Nappe (Prinzhofer, 1981, as cited in Cluzel, Maurizot, et al., 2012).

The Peridotite Nappe is in places associated with a metamorphic sole consisting of meta-basalt at amphibolite grade with subordinate metasediments. These are generally interpreted to form during subduction initiation at or near a spreading ridge (Cluzel, Jourdan et al., 2012; Van Hinsbergen et al., 2015). Hornblende $^{40}Ar/^{39}Ar$ and zircon U-Pb dating of metamorphic sole amphibolites yielded ages of ~56 Ma (Cluzel, Jourdan et al., 2012). The closure temperature for Ar in hornblende is lower than for typical temperatures in amphibolite-facies sole rocks and thus the 56 Ma age dates cooling during sole exhumation, which is likely intrinsically related to the subduction initiation process (Van Hinsbergen et al., 2015). The subduction zone below the Peridotite Nappe therefore probably initiated within a few million years before 56 Ma.

Upon arrival of Norfolk Ridge at the trench and consequent obduction of the ophiolite, the western SW Pacific subduction zone terminated on New Caledonia. Timing of obduction initiation during the Late Eocene is constrained by the age of the youngest sediment on which the ophiolite was thrust (34.7–35 Ma, Cluzel et al., 2001). The end of obduction is constrained by postobduction plutons intruded into the Peridotite Nappe and its autochthonous basement. Ages of 27.5 and 24 Ma were obtained through U-Pb dating of magmatic zircons of these postobduction granitoids (Paquette & Cluzel, 2007).

Extensive geochemical analysis by Ulrich et al. (2010) suggested that the mantle section of the Peridotite Nappe underwent two melting stages. The Peridotite Nappe consists of highly depleted harzburgites with U-shaped bulk-rock rare-earth element patterns, indicative of a forearc environment. However, lherzolites are enriched with spoon-shaped light rare earth elements and melts from these lherzolites are geochemically similar to some of the mid-ocean ridge basalts from the underlying Poya Terrane that were offscraped from the oceanic crust that subducted below the Peridotite Nappe prior to its obduction. Therefore, it is inferred that the Peridotite Nappe formed in the same oceanic basin as the Poya Terrane (Ulrich et al., 2010). A second melting stage in a forearc environment led to the ultradepletion of harzburgites that now form the bulk of the nappe. The geochemical signature of the Peridotite Nappe and overlying gabbronorite cumulates are indicative of a suprasubduction zone history (Marchesi et al., 2009; Ulrich et al., 2010).

4.2.3. D'Entrecasteaux Zone

The D'Entrecasteaux zone is an arch-shaped ridge connecting northern New Caledonia to central New Hebrides and its northeastern extension is currently subducting along the New Hebrides Trench (Figure 2). The ridge separates D'Entrecasteaux Basin to the northwest from North Loyalty Basin to the southeast. Bougainville Guyot is a seamount located at the eastern end of the South D'Entrecasteaux chain. The oldest rock dredged from this guyot is a volcanic breccia of Middle Eocene age (42–40 Ma), based on age determination from planktonic nanofossil content in the chalky matrix (Collot et al., 1992). K/Ar dating of volcanic rocks of the guyot yielded an age of 37 ± 0.1 Ma (Baker et al., 1994). Extensive geochemical analysis indicate an island arc tholeiite signature, with a negative Nb anomaly indicative of subduction-related magmatism (Baker et al., 1994). Based on these data, the D'Entrecasteaux zone is generally viewed as an Eocene island arc and the northward, intraoceanic, continuation of Loyalty Ridge (Crawford et al., 2003).

4.2.4. Loyalty Ridge

Seismic reflection and swath bathymetry data indicate that Loyalty Ridge is composed of spaced seamounts that are covered by a thick carbonate layer (Cluzel, Maurizot et al., 2012; Lafoy et al., 1996). The size and spacing (~70 km, Eissen et al., 1998) of the seamounts are typical of an island arc, but due to lack of basement outcrop the geology of the ridge is still poorly known (Cluzel, Maurizot et al., 2012; Lafoy et al., 1996). Despite the lack of data, most authors consider Loyalty Ridge to be an Eocene Island arc (e.g., Baker et al., 1994; Cluzel et al., 2001; Crawford et al., 2003; Maillet et al., 1983; Paquette & Cluzel, 2007; Schellart et al., 2006), partly based on continuity of the submarine structure and evidence from the Bougainville guyot as described above.

4.2.5. Three Kings Ridge

Three Kings Ridge is considered to represent a remnant of a volcanic arc, but both west-facing (e.g., Kroenke & Eade, 1982) and east-facing (e.g., Davey, 1982) arcs have been proposed. More recent work based on forearc boninites dredged to the immediate west of Three Kings Ridge suggests that it was the volcanic arc above an east-dipping subduction zone. $^{40}Ar/^{39}Ar$ ages between 37 and 30 Ma were obtained from plagioclase separates of these dredge samples (Bernardel et al., 2002). The 37 Ma boninite is interpreted to mark the start of subduction along Three Kings Ridge (Whattam et al., 2006, 2008). A 26 Ma $^{40}Ar/^{39}Ar$ age of biotite in volcanic breccia recovered from the western slope of Three Kings Ridge (Mortimer et al., 1998) is interpreted to represent the last stages of east-dipping subduction (Whattam et al., 2006).

Table 2
Plate IDs and Their Associated Plate Names as Used in the Reconstruction

Plate ID	Plate name
801	Australia
802	East Antarctica
804	West Antarctica
806	New Zealand north of Alpine Fault
813	Campbell Plateau, including New Zealand south of Alpine Fault
821	Tonga Ridge
823	Lau Ridge
824	Suture Vitiaz Trench
825	Fiji
827	New Hebrides Trench and North Fiji Basin
833	Lord Howe Rise
834	Norfolk Ridge
835	Three Kings Ridge
836	Coral Sea
837	Kermadec Ridge
838	Northwest South Fiji Basin
839	East South Fiji Basin
844	North Loyalty Basin, including Loyalty Ridge and New Caledonia
855	Southeast North Loyalty Basin
856	Colville Ridge
868	Challenger Plateau
901	Pacific

5. Reconstruction

5.1. Reconstruction Protocol

We now integrate the geological constraints described above into our plate kinematic restoration, which we made in the freely available software package GPlates (www.gplates.org; Boyden et al., 2011). GPlates-format shape and rotation files that contain this restoration are available in the supporting information.

The reconstruction presented here provides relative plate motions in the southwest Pacific realm and is based purely on spreading directions and rates from published interpreted marine magnetic anomaly data and fracture zone-transform fault directions. We adopt the reconstruction hierarchy of data types of Boschman et al. (2014). This hierarchy defines the order in which quantitative data types are used, from lowest to highest levels of uncertainty. This reconstruction consists of the following two data types in decreasing order of certainty:

1. Ocean basin restorations. Magnetic anomaly data and transform faults/fracture zones provide the best constraints on relative plate motions. Spacing of magnetic anomalies quantifies the amount of movement and the direction of movement is quantified by the orientation of fracture zones.
2. Additional geological data, used in the following order: continental extension records, strike-slip faults, continental shortening records, and paleomagnetism. Dredge samples are used to identify offshore crustal type. Paleomagnetic analysis is used for rotations of continents that cannot be defined by magnetic anomalies. Rock samples that are dated by radiometric methods are used to obtain crustal ages of lithosphere that lacks magnetic anomalies.

The bulk of this reconstruction is based on ocean basin restorations from published magnetic anomaly and transform faults/fracture zone data. Geological data are only used for areas where magnetic anomaly data are not available, for example, for the Alpine Fault history of New Zealand and the New Caledonia subduction zone. Ages of marine magnetic anomalies are based on the timescale of Ogg (2012).

The Antarctic circuit as described in section 2 is used as a starting point for our SW Pacific reconstruction. Plate motions between the five major tectonic plates (AUS, eANT, wANT, PAC, and LHR) in the Antarctic circuit are based on previously published rotation poles (Table 1) most of which are used in the global plate model of Müller et al. (2016). All plate motions east of LHR are based on the geological and kinematic constraints described in section 4 (see Table 2 for plate names and IDs). We use previously published finite rotation poles where possible. A few rotations are computed within *GPlates*, about which our choices are explained in section 4.2.

5.2. Tectonic Model of the Southwest Pacific

A summary of the reconstruction is found in Table 3 and snapshots at selected times are provided in Figure 10. Time slices are chosen based on proposed or observed important events in the SW Pacific kinematic history. At the start of our reconstruction (83 Ma) the five major tectonic plates (AUS, eANT, wANT, LHR, and PAC) were still assembled, but Gondwanaland breakup had commenced. Australia had started moving away from Antarctica around 90 Ma, but spreading was still very slow (Tikku & Cande, 1999, 2000; Whittaker et al., 2007, 2013; Williams et al., 2011). Also, some extension has taken place in the West Antarctic Rift system (Matthews et al., 2015; Spiegel et al., 2016).

Based on the finite rotation poles of Wright et al. (2015, 2016), there is an overlap between Campbell Plateau and the Marie Byrd Land sector of Antarctica. Because we put the unconstrained boundary between PAC and LHR between Challenger Plateau and LHR, the poles of Wright et al. (2015, 2016) also cause an overlap between Challenger Plateau and LHR. With spreading along Tasman Ridge and Pacific-Antarctic Ridge since 83.6 Ma, the overlap between Challenger Plateau and LHR is removed by a short

Table 3
Summary of Constraints and Amount of Motion Predicted by Our Model

Timing	Observation	Type of data used	References	Amount of motion predicted by our model
83.6–52.0 Ma	Tasman Sea spreading	Magnetic anomalies, fracture zone data	Gaina et al., 1998; Seton et al., 2012	Ranging from 800 km in the northernmost Tasman Sea to 1,200 km in the southernmost Tasman Sea
83.6 Ma to present	Southeast Indian Ridge spreading	Magnetic anomalies, fracture zone data, continent-ocean boundary constraints	Cande & Stock, 2004; Whittaker et al., 2013	3,000 km
83.6 Ma to present	Pacific-Antarctic Ridge spreading	Magnetic anomalies, fracture zone data	Croon et al., 2008; Wright et al., 2015, 2016	Ranging from 1,500 km in the west to 1,900 km in the east northeast-southwest extension between 83.6 and 45 Ma, and an additional 1,500 km to 2,200 km northwest-southeast extension between 45 Ma and present
100–26.3 Ma	West Antarctic Rift system extension	Magnetic anomalies, fracture zone data	Cande & Stock, 2004; Granot et al., 2013a; Matthews et al., 2015	100 km
83.6–56.0 Ma	Extension in Fairway-Aotea and New Caledonia Basins	Bathymetry, magnetic anomalies, gravity data and multichannel seismics	Wood & Woodward, 2002; Lafoy et al., 2005; This study	160 km
63.0–52.0 Ma	Coral Sea spreading	Magnetic anomalies, fracture zone data	Gaina et al., 1999	Ranging from 330 km in the west to 500 km in the east
60.0–30.0 Ma	New Caledonia subduction	Geologic data of the New Caledonia ophiolite (metamorphic sole and postobduction plutons)	Paquette & Cluzel, 2007; Schellart, 2007; Schellart et al., 2009; Cluzel, Jourdan et al., 2012; This study	Ranging from 670 km at the northernmost part of the subduction zone to 300 km in the south
43.4–35.0 Ma	Back-arc extension in North Loyalty Basin	Magnetic anomalies, fracture zone data	Sdrolias et al., 2003	750 km
40.0–24.0 Ma	Macquarie Ridge Spreading	Magnetic anomalies, fracture zone data	Keller, 2004	Ranging from 550 km in the west to 250 km east, followed by 600 km dextral strike-slip motion since 24 Ma.
45.0 to 30.0 Ma to present	Tonga-Kermadec subduction	Kinematic reconstruction	This study	Total amount of subduction until present day ranges from 1,700 km in the south to 3,500 km in the north
27.4–15.0 Ma	Back-arc extension in South Fiji Basin	Magnetic anomalies, fracture zone data, Ar/Ar dating of dredge samples	Sdrolias et al., 2003; Mortimer et al., 2007; Herzer et al., 2009, 2011	Ranging from 950 km in the northernmost South Fiji Basin to 350 km in the southernmost South Fiji Basin
24.0–15.0 Ma	Back-arc extension in Norfolk Basin	Fracture zone data, bathymetry, Ar/Ar dating of dredge samples.	Sdrolias et al., 2004; Mortimer et al., 2007; Herzer et al., 2009, 2011; This study	270 km in the north and 170 km in the south of Norfolk Basin
10.0 Ma to present	New Hebrides subduction	Geological data	Crawford et al., 2003	Total amount of subduction ranges from 400 km at the northern end of the subduction zone to 1,000 km at the southern end.
10.0 Ma to present	Spreading in North Fiji Basin	Magnetic anomalies, fracture zone data	Yan & Kroenke, 1993	Ranging from 400 km in the northwest to 1,000 km in the southeast of North Fiji Basin
10.0–3.0 Ma	Counterclockwise rotation of Fiji	Paleomagnetism	Taylor et al., 2000	135° degree of counterclockwise rotation
7.0 Ma to present	Back-arc extension in Lau Basin	Magnetic anomalies	Yan & Kroenke, 1993	Ranging from 500 km in the north to 200 km in the south of Lau Basin
7.0 Ma to present	Back-arc extension in Havre Trough	Magnetic anomalies	Yan & Kroenke, 1993; This study	200 km

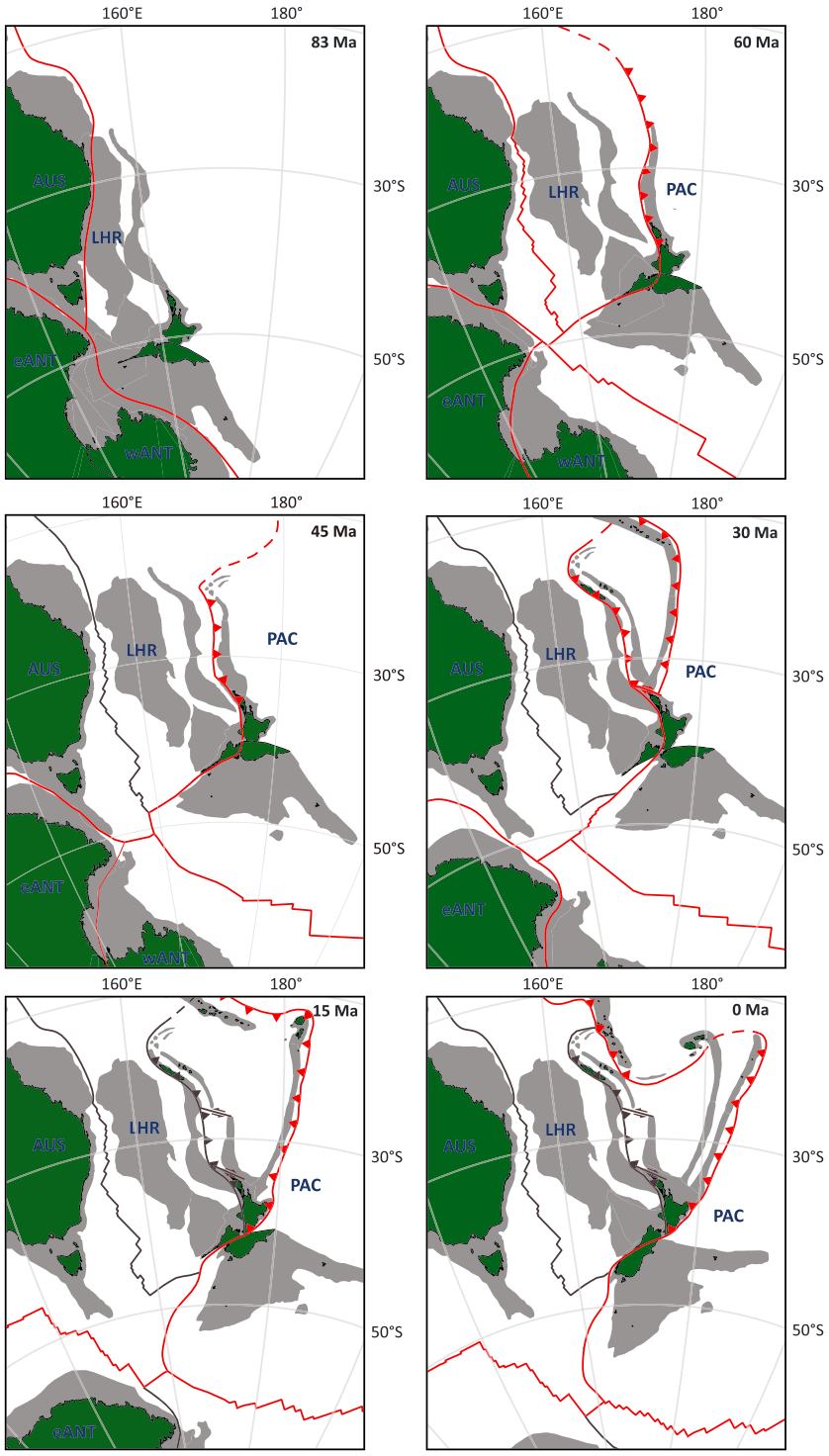

Figure 10. Paleogeographic snapshots of the kinematic reconstruction at selected time slices in an Australia fixed frame. 83 Ma: Start of the reconstruction; 60 Ma: start of New Caledonia subduction; 45 Ma: oldest possible, and frequently mentioned, age of Tonga-Kermadec subduction zone; 30 Ma: end of New Caledonia subduction, youngest possible age of Tonga-Kermadec subduction zone initiation and start of Norfolk and South Fiji Basin back-arc spreading; and 15 Ma: end of Norfolk and South Fiji Basin back-arc spreading.

transtensional phase (83.6–80 Ma). The transtensional phase is also predicted by Gaina et al. (1998) and Van de Beuque et al. (2003).

Following the age interpretation of Lafoy et al. (2005), extension is adopted in Fairway-Aotea Basin and New Caledonia Basin between 85 and 56 Ma. Based on the 30% crustal thinning estimated for the Fairway Basin (Lafoy et al., 2005; Wood & Woodward, 2002), we speculatively use a total of 50% extension in the combined Fairway-Aotea and New Caledonia basins.

Based on the 56 Ma age of the metamorphic sole of the ophiolite (Cluzel, Jourdan et al., 2012), we infer that northeast-directed subduction along the New Caledonia subduction zone started at 60 Ma (Figure 10). This age corresponds to a change in Australia absolute plate motion from north to east-northeast (using the global moving hot spot reference frame of Doubrovine et al., 2012), changing relative plate motion between Pacific and Norfolk Ridge from strike-slip to convergent.

Subduction along the New Caledonia Trench led to back-arc extension in the North Loyalty Basin between 44 and 35 Ma. We used the finite rotation poles of Sdrolias et al. (2003) for the opening of this basin and restored the northern part of the basin (i.e., D'Entrecasteaux zone) relative to the southern part of the basin. This leads to northwestwards directed trench rollback and arc-parallel extension at Loyalty Arc in the reconstruction, which is also predicted by the tectonic model of Sdrolias et al. (2003). Subduction along the New Caledonia Trench ended with final obduction of the New Caledonia ophiolite at around 30–25 Ma (Paquette & Cluzel, 2007). Slab break-off is thought to have occurred around 25 Ma in the New Caledonia, Three Kings Ridge and Northland regions (Schellart, 2007; Schellart et al., 2009; Sevin et al., 2014). A 30-Ma age for the end of New Caledonia subduction is incorporated in our model.

Subduction at the New Caledonia Trench consumed the South Loyalty Basin. The geometry of the South Loyalty Basin is modeled by assuming that the basin was part of PAC until New Caledonia was partially subducted. This means that in our Gplates plate circuit the Three Kings Ridge is attached to PAC until 60 Ma, as Three Kings Ridge forms the plate boundary between PAC and South Loyalty Basin during subduction at New Caledonia subduction zone. Subduction at the New Caledonia subduction zone is subsequently modeled to have occurred at a constant rate from the position of Three Kings Ridge at 60 Ma until the arrival of the Norfolk Ridge at 30 Ma (Figure 10).

During the final stages of obduction at the New Caledonia subduction zone, extension commenced in South Fiji Basin (~28 Ma, Herzer et al., 2011) and Norfolk Basin (~24 Ma, Sdrolias et al., 2004). Opening of South Fiji Basin is modeled using finite rotations of Sdrolias et al. (2003), using the reinterpreted ages of Herzer et al. (2011). Opening of the South Fiji Basin occurred in a back-arc setting to the Tonga-Kermadec subduction zone, where subduction had initiated by that time.

Spreading in Norfolk Basin was concurrent with spreading in South Fiji Basin and resulted in eastward migration of Three Kings Ridge. We restore Three Kings Ridge back to its original position by lining it up with the present-day position of Loyalty Ridge, along strike of the Cook Fracture Zone. This results in a 270-km southeastwards displacement of northern Three Kings Ridge between 24 and 15 Ma. Some 170 km of extension is predicted in southern Norfolk basin, and transpressive motion occurs on the Veining Meinesz Fracture Zone, which is in agreement with Herzer and Mascle (1996).

The 15 Ma end of extension in both basins is based on age interpretations of Mortimer et al. (2007) and Herzer et al. (2009, 2011). The rollback of the Lau-Colville Ridge associated with concurrent back-arc spreading in Norfolk and South Fiji basins is estimated to be about 500 km at the southern Colville Ridge and up to 700 km at the northern Lau Ridge.

The Ontong Java Plateau arrived at the Vitiaz Trench during the Early to Middle Miocene, resulting in a subduction polarity reversal (Auzende et al., 1995; Knesel et al., 2008; Petterson et al., 1997; Quarles van Ufford & Cloos, 2005). This led to spreading in North Fiji Basin from 10 Ma, clockwise rotation of New Hebrides arc (Yan & Kroenke, 1993) and anticlockwise rotation of the Fiji Plateau (Taylor et al., 2000).

Soon after 7 Ma, the Lau Basin-Havre Trough back-arc basin started opening (Ruellan et al., 2003), which led to splitting of the Tonga-Kermadec Ridge from the Lau-Colville Ridge. Extension in the Lau Basin is reconstructed using the finite rotation poles of Yan and Kroenke (1993). Motion in Havre Trough is reconstructed by closing the basin at 7 Ma and aligning the Kermadec Ridge with the position of the Tonga Ridge at that

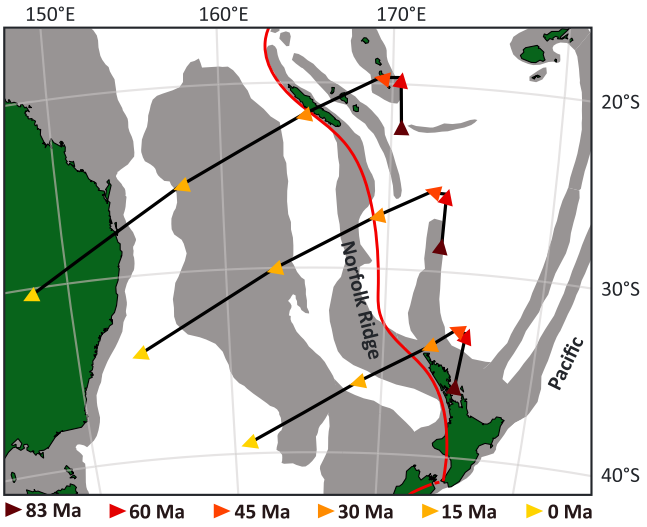

Figure 11. 83 Ma—Present day motion paths of three points on the Pacific plate relative to Norfolk Ridge, yielding maximum convergence during opening of the Tasman Sea between 83 and 52 Ma. Between 83 and 45 Ma, there is only minor relative plate motion. Around 45 Ma, there is a sharp increase in overall convergence, whereby convergence rates are less in the south than in the north.

time. Constant spreading since 7 Ma is assumed, which leads to a good fit with the reconstructed motion of the southern end of the Tonga Ridge.

Rollback of Tonga Ridge since 7 Ma occurred in a clockwise fashion, which means that the amount of rollback is greatest in the north. There the amount of rollback exceeds 550 km, while it is only about 250 km at the southern Tonga Ridge. Rollback of the Kermadec Ridge, on the contrary, is reconstructed to have occurred parallel to Colville Ridge, with approximately 230 km of rollback along the entire length of the ridge.

Altogether, SW Pacific underwent several stages of basin opening and southeastward-directed trench rollback since 28 Ma. Our reconstruction predicts a total amount of trench rollback of approximately 1,300 km at the northern end of the subduction system, decreasing southwards to about 700 km just northeast of North Island, New Zealand.

5.3. Pacific-Norfolk Ridge Convergence

Based on our choice of the Antarctic plate circuit and its associated finite rotations, our reconstruction yields a prediction of the amount of convergence between Pacific plate and Norfolk Ridge. Norfolk Ridge is chosen as a reference, as it is the most easterly element that moves independent of Australia until the Late Oligocene back-arc spreading in Norfolk and South Fiji basins started. Therefore, relative motion between Pacific plate and Norfolk Ridge yields the maximum amount of convergence.

Before onset of subduction at the New Caledonia trench (60 Ma), motion between Pacific plate and Norfolk Ridge is mainly strike-slip (Figure 11). Relative motion between 83 and 60 Ma is mainly left lateral, except for an interval between 72 and 65 Ma, when motion is right lateral with a divergent component. At 60 Ma, the relative motion becomes convergent, but this motion remains small (Figure 11). Between 60 and 51 Ma the total amount of net convergence along Norfolk Ridge is estimated to be about 100 km, which corresponds to an average convergence rate of ~14 mm/year. Between 51 and 45 Ma, relative motion is again predicted to be mainly left-lateral strike slip, with a diverging component southward of 30°S.

At 45 Ma, absolute Pacific plate motion changed from north-northeast to northwest, which caused rapid convergent motion between the Pacific plate and Norfolk Ridge (Figure 11), by this time part of the Australian plate. Since 45 Ma, relative Pacific-Australian plate motion has been fairly constant in both direction and rate. Relative motion has been directed mainly west to southwestwards, with a small interval between 34 and 30 Ma of more south to southeastwards directed motion at southern latitudes (south of ~30°S). Rate of convergence increased at 26 Ma from an average of ~30 mm/year between 45 and 26 Ma (~575 km in 19 Myr, latitude 20°S to 22°S), to an average of ~68 mm/year since 26 Ma (~1,775 km in 26 Myr, latitude 22°S to 28°S). From 60 Ma onwards, our plate circuit predicts a total amount of Pacific-Norfolk Ridge convergence of ~3,000 km at the northernmost end of the Tonga-Kermadec subduction system and ~1,500 km at the southern end. Convergence estimates since 30 Ma are ~2,200 km and ~1,000 km for the northern and southern ends of the Tonga-Kermadec Trench, respectively. This means that, including trench-rollback of the Lau-Colville and Tonga-Kermadec ridges, a total of at least 3,500 and 1,700 km of subduction are predicted for the northern and southern ends of the Tonga-Kermadec Trench, respectively.

6. Discussion

6.1. South Loyalty Basin Extension and Implications for Tonga-Kermadec Trench Evolution

For analysis of the onset of subduction along the Tonga-Kermadec Trench, the history of the oceanic lithosphere consumed by the New Caledonia subduction zone, referred to as South Loyalty Basin oceanic lithosphere (e.g., Cluzel et al., 2001; Cluzel, Jourdan et al., 2012; Matthews et al., 2015; Schellart et al., 2006), is of importance. The opening history of this basin needs to be discussed as it may have influenced evolution

of the Tonga-Kermadec Trench. We acknowledge that the age and geodynamic context of spreading within the inferred South Loyalty Basin is uncertain. Small relics of the South Loyalty Basin occur in the small basin nestled between Grande Terre and Loyalty Islands (Figure 2), and data from this basin are scarce. The only direct observations come from the Poya Terrane that was accreted below the New Caledonia ophiolite. Poya Terrane rocks are thought to have once floored South Loyalty Basin (e.g., Cluzel et al., 2001; Cluzel, Jourdan, et al., 2012).

The occurrence of radiolarian faunas in pelagic red chert and siliceous siltstone interbedded with Poya Terrane basalt (Cluzel et al., 2001) has led many authors to assume a Late Cretaceous to earliest Eocene (85–55 Ma) opening history of South Loyalty Basin (e.g., Matthews et al., 2015; Schellart et al., 2006). On the other hand, based on geodynamic modeling combined with geological and geophysical observations, Matthews et al. (2011) postulated that the Panthalassic Trench during the Mesozoic was likely located approximately 1,000 km east of the eastern Gondwana margin. They thus implied that South Loyalty Basin would have been in a back-arc position at that time, consistent with the geochemical fingerprint of some of Poya basalt as back-arc basin tholeiite (Cluzel et al., 2001; Eissen et al., 1998) and would have had an age of 140–120 Ma. This basin would then have opened during rollback of the southwest Panthalassa subduction zone that consumed the Phoenix plate (Matthews et al., 2012; Seton et al., 2012).

Opening of South Loyalty Basin is not included in our reconstruction due to an absence of direct kinematic constraints. However, its opening history has significant implications for tectonic history of the SW Pacific region and evolution of the Tonga-Kermadec Trench. Two timeframes for opening of this basin has led to two different models of SW Pacific tectonic evolution.

If we assume for the moment that South Loyalty Basin opened between 140 and 120 Ma as a back-arc basin to the southwest Panthalassic Trench, it would have opened above the long-lived subduction zone that must have existed along the eastern margin of Gondwana and consumed Phoenix plate's oceanic crust beneath Panthalassa Ocean (Matthews et al., 2012; Seton et al., 2012). Competing models for the timing of subduction cessation exist, and both 105 and 100 Ma (e.g., Davy et al., 2008; Matthews et al., 2012; Sutherland & Hollis, 2001) and 86- to 80-Ma ages have been inferred (e.g., Seton et al., 2012; Worthington et al., 2006). Both suggested timeframes for cessation of subduction allow opening of South Loyalty Basin as a back-arc basin to the Panthalassic Trench between 140 and 120 Ma. In this scenario no subduction zone is required by the plate circuit or the geological record of the SW Pacific region between the cessation of subduction (sometime between 105 and 80 Ma) and onset of New Caledonia subduction around 60 Ma. In this case, there is no reason to assume that the Tonga-Kermadec Trench was active during the Early Cenozoic.

The alternative, in which South Loyalty Basin opened between 85 and 60 Ma, would allow a scenario where its spreading ridge became inverted around 60 Ma to form the New Caledonia Trench. Schellart et al. (2006) estimated that the South Loyalty Basin had a minimum east-west width of 750 km. In the absence of net PAC-LHR convergence, opening of South Loyalty Basin would require subduction of PAC and rollback of its trench over the 750 km width of the South Loyalty Basin, which, logically, would be accommodated along the former Panthalassic Trench (e.g., Cluzel, Maurizot et al., 2012; Schellart et al., 2006; Ulrich et al., 2010).

There is no geological evidence for any significant extension in the SW Pacific region between 60 and 30 Ma, and there was barely any plate convergence until 45 Ma. What little plate convergence did occur between the ~60-Ma initiation of subduction recorded by the New Caledonia ophiolite and the 45 Ma onset of significant Pacific-Australia convergence must have been accommodated along the New Caledonia Trench. If there had been subduction at the former Panthalassic Trench until 60 Ma, we consider it most likely that the slab broke off at 60 Ma and subduction restarted at a later date. Seismic tomographic images reveal anomalies in the mantle deeper than the Tonga-Kermadec slab below the SW Pacific and Australian regions that likely represent subducted Phoenix plate lithosphere, but these have not been interpreted in detail given general lack of field observations of geological records associated with Mesozoic Phoenix subduction north of New Zealand (Van der Meer et al., 2018).

In summary, in both scenarios of opening of South Loyalty Basin, it is very unlikely that the current Tonga-Kermadec Trench has been continuously active since the Cretaceous. In the 140- to 120-Ma opening scenario, subduction ceased before 80 Ma (e.g., Seton et al., 2012). In the 85- to 60-Ma opening scenario subduction continued, entirely driven by rollback in absence of plate convergence (Matthews et al., 2015; this study), followed by stagnation of subduction and slab break-off. We therefore consider scenarios inferring the

occurrence of subduction at the Tonga-Kermadec Trench throughout the Late Cretaceous to Paleogene (e.g., Schellart et al., 2006) as unlikely. The present extent of slab subducted at the Tonga-Kermadec tTrench must date from subduction initiation during the Cenozoic.

6.2. Age of Tonga-Kermadec Subduction Initiation Versus New Caledonia Subduction Termination

We now combine our kinematic reconstruction with seismic tomographic constraints on mantle structure to estimate the age of initiation of subduction at the Tonga-Kermadec Trench as a function of evolution of the New Caledonia Trench.

In our reconstruction, the amount of Pacific-Norfolk ridge convergence before 45 Ma is minimal (~100 km between 60 and 45 Ma, which is within typical uncertainties of marine magnetic anomaly reconstructions). We consider it unlikely that this small amount of convergence was partitioned between two subduction zones. Recently, Sutherland et al. (2017) suggested that thrusting inferred from seismic sections from the Tasman Sea (Reinga Basin, Lord Howe Rise, New Caledonia Trough and Tasman Abyssal Plain) and dated 53–48 Ma resulted from subduction initiation at the Tonga-Kermadec Trench, assuming that initiation there occurred simultaneously with subduction initiation below the Philippine Sea Plate at the Marianas Trench. Such Eocene shortening was also reported from Fairway Basin located west of New Caledonia (Rouillard et al., 2017). Both Lord Howe Rise and Fairway Basin were part of the Australian plate, separated from the Tonga-Kermadec Trench by a plate boundary (the New Caledonia Trench) and from the Marianas Trench by another plate boundary (Melanesian Trench). Therefore, interpreting the shortening in Tasman Sea basins as an indication of subduction initiation along either trench (e.g., Rouillard et al., 2017; Sutherland et al., 2017) is not straightforward. This Eocene shortening may instead more likely reflect upper crustal processes emanating from the New Caledonia plate boundary and subduction there, or be related to termination of Australia plate subduction at Papua New Guinea and subsequent slab break-off following obduction (see Schellart & Spakman, 2015). Furthermore, the kinematic rationale why subduction initiation of the Pacific Plate beneath the Philippine Sea Plate at 52 Ma (e.g., Ishizuka et al., 2011) should be contemporaneous with Pacific plate subduction below the Australia plate is unclear, particularly because Australia-Philippine Sea Plate motions are essentially unconstrained. As existence of the New Caledonia subduction zone since 60 Ma has been inferred from geological evidence, the maximum feasible age of the Tonga-Kermadec subduction zone is 45 Ma, corresponding to the onset of significant PAC-LHR convergence.

After the end of subduction at the New Caledonia Trench, all plate convergence must have been accommodated at the Tonga-Kermadec Trench. Schellart (2007) and Schellart et al. (2009) suggested a 30-Ma age for subduction cessation at New Caledonia and a 25-Ma age for final slab detachment (Sevin et al., 2014). This suggests that subduction at the Tonga-Kermadec Trench started at earliest between 30 and 45 Ma.

During the existence of the New Caledonia subduction zone (60–30 Ma), our reconstruction predicts about 700, 450, and 225 km of Pacific-Norfolk Ridge convergence at New Caledonia, at northern Three Kings Ridge and at Northland, respectively (Figure 11). Based on seismic tomography, Schellart et al. (2009) interpreted the South Loyalty slab to contain 600–900 km of lithosphere. Our analysis of the UU-P07 tomographic model (Amaru, 2007) shows that the current anomaly has a length of about 300 km from bottom to top (Figure 7), but it may well have been thickened during its transition into the lower mantle (Schellart et al., 2009). Typical thickening factors of 2–3 for slabs in the upper 1,000 km of the lower mantle (Hafkenscheid et al., 2006; Van der Meer et al., 2018) bring our observation in line with the interpretation of Schellart et al. (2009). This means that the 700 km of 60- to 30-Ma Pacific-Norfolk Ridge convergence inferred from our reconstruction may have been completely accommodated at the New Caledonia subduction zone, which then consumed the entire, ~700 km E-W width of the South Loyalty Basin (Schellart et al., 2006).

Comparison of our kinematic reconstruction with constraints from seismic tomography thus implies that subduction at the Tonga-Kermadec Trench probably started as late as ~30 Ma. Subducted lithosphere volumes from seismic tomography are obviously subject to uncertainty and hence we cannot rule out occurrence of some subduction at the Tonga-Kermadec Trench between 45 and 30 Ma. Nonetheless, our study indicates that if Tonga-Kermadec subduction started sometime between 45 and 30 Ma, it accommodated no more than a few hundred kilometers of subduction. Even if the New Caledonia slab has not experienced any thickening, which is highly unlikely (Van der Meer et al., 2018), the Tonga-Kermadec subduction zone could only have accommodated the remaining 400 km of predicted convergence. The bulk of the present

Tonga-Kermadec slab must therefore have formed after ~30 Ma. An implication is that back-arc spreading in Norfolk and South Fiji basins since 28 Ma occurred above the Tonga-Kermadec subduction zone.

Additional constraints on the timing and evolution of the New Caledonia and Tonga-Kermadec subduction zones comes from New Zealand, where both subduction zones terminate in the south, and its geological record also helps to constrain the age of initiation of these systems. Schellart et al. (2006) proposed that the southern end of the New Caledonia Subduction Zone lay immediately northeast of northern North Island from about 40 Ma and subsequently rolled back, leading to emplacement of Northland Allochthon during 25–21 Ma. While there are no data about which we are aware to constrain a 40-Ma age of subduction initiation northeast of Northland and a ~60 Ma initiation consistent with New Caledonia would hence be more likely, substantial Late Eocene-Early Oligocene shortening occurred in Reinga Basin and margins of New Caledonia Basin to the west of northern Northland (Bache et al., 2012). It is possible, therefore, that the shortening required from kinematic data to be expressed in the Northland region (225 km, see above) was partitioned across a wide area associated with the emplacement of Northland Allochton—in part into the southern end of the subduction zone and in part into continental crust immediately to the west beneath Reinga Basin. Taranaki Basin lies south of Reinga Basin and recent analysis shows that the Middle to Late Eocene-Early Oligocene sedimentary section beneath northern Taranaki Basin, including Taranaki Peninsula, accumulated in a foredeep, the subsidence having been caused by westward over-thrusting of basement on Taranaki Fault (Kamp et al., 2017). Thus it appears that Eocene-Early Oligocene shortening expressed as subduction in the New Caledonia system transitioned into continental crust of northern New Zealand, initially via a zone of distributed deformation, before narrowing farther south into a paired thrust belt and foredeep in Taranaki Basin, where the shortening ended. The region south of Taranaki Peninsula, including South Island, lay south of the contemporary pole of rotation and hence Late Eocene-Early Oligocene plate boundary kinematics were manifest as continental rifting (Kamp, 1986; Furlong & Kamp, 2013) that then passed southward into Emerald Basin where seafloor spreading occurred during the Late Eocene-Oligocene (Keller, 2004).

The stratigraphy and structure of eastern North Island provide strong evidence for Early Miocene initiation of subduction along the Hikurangi Subduction Zone, which represents the southern part of the Tonga-Kermadec system. A comparatively thin (several hundred meters thick) Late Cretaceous and Paleogene succession, capped by Oligocene marl (Weber Formation), accumulated as bathyal deposits on a quiescent continental margin in eastern North Island (Field and Uruski, 1997). This sedimentation pattern changed dramatically during the Early Miocene with the emplacement of thrust sheets of the East Coast Allochthon (Stoneley, 1968) and with formation of localized basins (accretionary slope basins) in which thick (1–4 km) mud-dominated sequences accumulated (e.g., Field & Uruski, 1997; Mazengarb & Speden, 2000). The Early Miocene (23 Ma) initiation of subduction at the Hikurangi Margin is part of the development of a through-going Australia-Pacific plate boundary in New Zealand after about 23 Ma, including the Alpine Fault sector in South Island and the Puysegur subduction margin offshore to the southwest (Kamp, 1986; King, 2000; Sutherland, 1999). This 23-Ma timing of initiation of subduction at the Hikurangi margin constrains the minimum age of initiation of subduction along the southern Tonga-Kermadec system with which it is continuous.

6.3. Absolute Plate and Trench Motion Compared to Tomography

We illustrate absolute plate motions in the SW Pacific region using the global moving hot spot reference frame of Doubrovine et al. (2012) and test the resulting positions of the reconstructed trenches against seismic tomographic constraints on slab locations. We compared the location of the New Caledonia subduction zone when subduction there ended at 30 Ma to the current location of the South Loyalty Basin slab in the mantle as identified by Schellart et al. (2009). Our reconstruction predicts a location of the New Caledonia subduction zone during slab detachment that corresponds very well to the present-day location of the slab. At 30 Ma the trench is located just south of the slab, consistent with north-east dipping subduction at the New Caledonia subduction zone (Figure 12). Since 30 Ma, the suture of the New Caledonia trench, including the associated ophiolites and extinct volcanic arc, moved ~1,400 km northwards relative to the mantle to its current location, leaving the detached slab behind in the mantle (Figure 12). This offset of the New Caledonia Ophiolite from the South Loyalty Basin slab is thus consistent with the absolute plate motion predictions of Doubrovine et al. (2012). Similarly, Schellart and Spakman (2015) showed that the Lake Eyre slab below

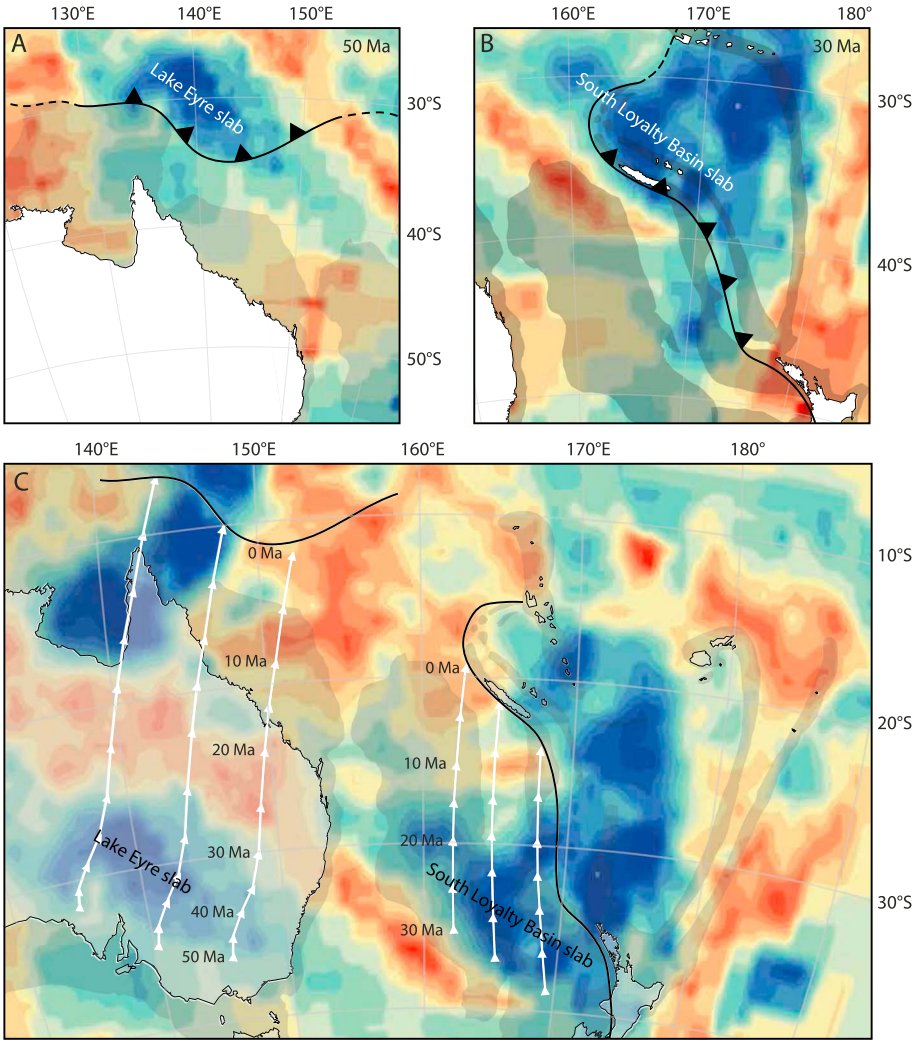

Figure 12. Reconstruction snapshots in the absolute plate motion frame of Doubrovine et al. (2012) and tomographic images at a depth of 1,050 km, based on the UU-P07 tomographic model (Amaru, 2007). The limits of the color scale used in this figure are the same as for Figure 5. The 1,050 km depth is selected as it reveals the extent of all three slabs very clearly. (a) Reconstructed location of the New Guinea-Pocklington subduction zone at 50 Ma above the Lake Eyre slab. (b) Reconstructed location of the New Caledonia subduction zone at 30 Ma above the South Loyalty Basin slab. (c) Present-day configuration of the SW Pacific. White lines indicate motion paths of the respective trenches relative to the mantle since inferred detachment of their associated slabs. White arrows in 5-Myr intervals.

southern Australia is also consistent with the predictions of the Doubrovine et al. (2012) global moving hot spot reference frame. In the same absolute motion frame, the Tonga-Kermadec analysis shows, however, no offset between the present-day trench and the associated anomaly imaged by seismic tomography because it is still attached to the Pacific plate. The entire slab is located to the west of the present-day trench along the full length of the trench (Figure 6). The location of the slab is one that is to be expected when viewed in an Australia-fixed reference frame (Figure 13), or, by implication, the Tonga-Kermadec slab must essentially have shared all or a large part of the northward absolute plate motion component of the Australian and Pacific plates. Such a shared component is not evident at all in a local relative plate motion frame (Spakman et al., 2018) and puts a novel constraint on Pacific absolute plate motion independent of the data and assumptions that determined the GMHRF frame of Doubrovine et al. (2012).

6.4. Trench-Parallel Slab Dragging Component of the Tonga-Kermadec Subduction

The lack of offset between the Tonga-Kermadec Trench and the imaged deep portions of Pacific plate slab has important implications. Subduction at the Tonga-Kermadec Trench is the result of E-W (normal)

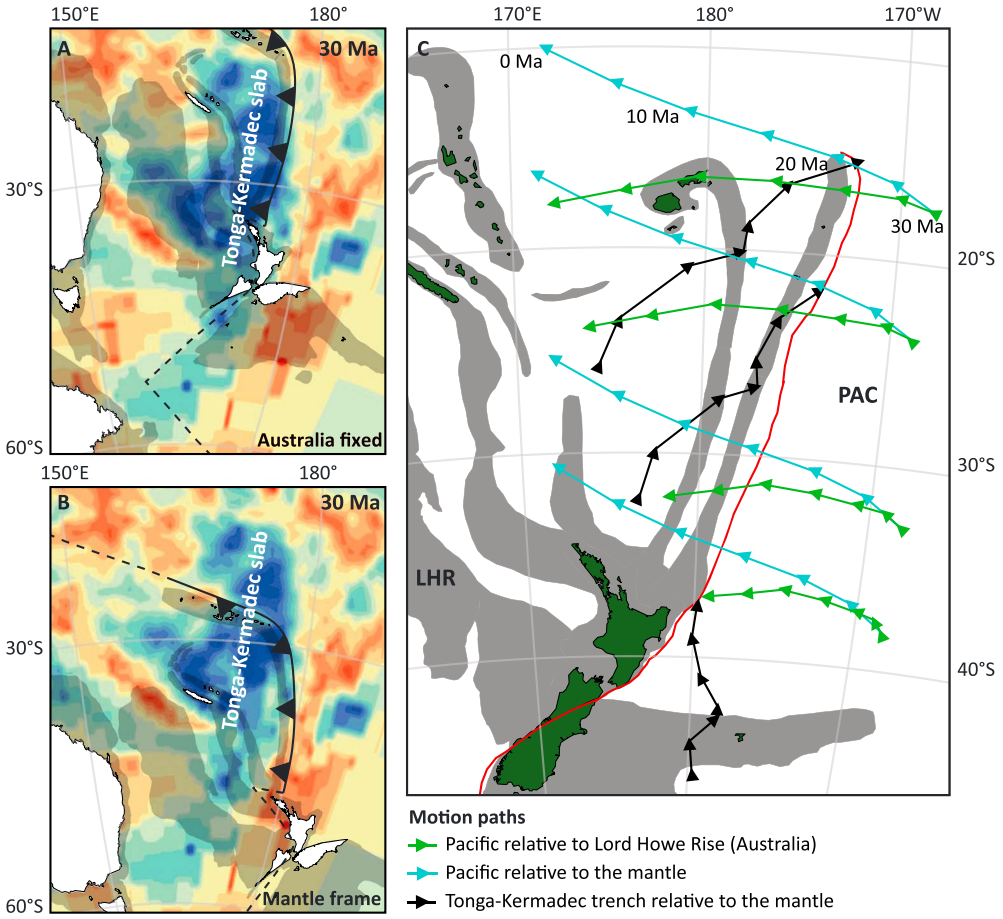

Figure 13. 30 Ma reconstruction in an (a) Australia-fixed reference frame and (b) mantle-reference frame, both with seismic tomographic images at 1,050 km depth, based on the UU-P07 tomographic model (Amaru, 2007). The limits of the color scale used in this figure are the same as for Figure 5. Whilst the image of Figure 13b shows the actual position of the Tonga-Kermadec Trench at 30 Ma, the fit between the tomography and the trench in Figure 13a is much better (see also Figure 6). This suggests that the Tonga-Kermadec slab must have moved northward through the mantle during its subduction history. This is illustrated in Figure 13c: Motion paths of Pacific plate relative to Lord Howe Rise (part of Australian plate; green), Pacific plate relative to the mantle (blue) and the Tonga-Kermadec Trench relative to the mantle (black) since 30 Ma (arrows in 5-Myr intervals) using the reconstruction shown in this paper placed in a mantle reference frame (Doubrovine et al., 2012).

convergence between Australia and Pacific plates. Concurrently, both plates underwent rapid (~7 cm/year) northwards absolute plate motion over the course of the 30 m.y. existence of the Tonga-Kermadec subduction zone. The northernmost part of the Tonga-Kermadec Trench thus moved ~1,850 km northeastwards relative to the mantle since 30 Ma, of which the northward absolute motion component was ~1,200 km. The southernmost Kermadec trench has moved ~1,200 km northward since 30 Ma. As seismic tomography reveals that the entire slab is located west (and not southwest or south) of the present-day trench, the slab, while subducting, must have been subjected to lateral dragging by the Pacific plate through the mantle, nearly parallel to the strike of the trench, by at least 1,200 km, along with northward motion of the trench (Figure 13). Even more spectacularly, seismic tomography suggests that slab dragging was not only restricted to the upper mantle, but that the portion of the slab located in the upper part of the lower mantle also shows no southward offset relative to the present-day trench (Figures 6 and 13).

The occurrence of slab dragging on such a large scale is a noteworthy discovery, especially considering the large volume of the slab and must result from the sum of dynamic processes forcing Pacific and Australian plate motions, in which northward motion at the edge of both plates plays an important role. The potential role of long-term slab-parallel mantle flow exerting viscous coupling to the slab can be limited as long as slab dragging by the Pacific plate occurred predominantly trench-parallel. A preliminary modeling study

(Chertova et al., 2018) suggests that 25 Myr of slab-parallel upper and lower mantle flow of 3 cm/year may not have a very large effect on slab morphology, except for thickening of the slab edge on which the flow impacts, while if mantle flow is oblique to the slab larger slab deformation may occur such as strong out-of-plane deflections. The tomography image of the slab is too blurred to assess any slab morphology change due to internal deformation of the slab or to detect appreciable lateral shifts in lower mantle slab position of the order of a few hundred km. The observations from focal mechanisms of strong upper-mantle slab deformation made by Giardini and Woodhouse (1986) suggest, however, a significant effect of mantle resistance against slab dragging at least in the more recent evolution of subduction.

Our study shows that a very large slab that has penetrated the lower mantle has been subjected to rapid slab dragging. In the case of this Tonga-Kermadec subduction zone, slab dragging may have been facilitated by interaction of the slab with the relatively hot mantle surrounding the Samoan plume, visible as the hot colors in tomographic images (Figure 7) below and east of the slab, that may have weakened the mantle regionally (Chang et al., 2016; Druken et al., 2014). Nevertheless, our study demonstrates that even at fast and long subduction zones, slabs may undergo trench-parallel absolute motion that must be far-field driven. Slab dragging alters the force balance of subduction via mantle resistance against lateral slab transport, which may lead to slab deformation, buildup of mantle seismic anisotropy and unexpected slab-plate interactions. Slab dragging and its effects on deformation of lithosphere opens new avenues for geodynamic and tectonic research (Chertova et al., 2014; Spakman et al., 2018).

7. Conclusions

We report here a kinematic reconstruction of the SW Pacific region for the Late Cretaceous to Present Day to estimate when Tonga-Kermadec subduction started and to study how the Tonga-Kermadec slab responded to a dominant component of northward absolute plate motion of the down-going Pacific plate that was partly shared by the overriding plates. Our conclusions are summarized as follows:

1. There was no demonstrable Pacific-Lord Howe Rise plate convergence between ~85 and 60 Ma. If subduction occurred at a Tonga-Kermadec Trench during this interval, it must have balanced divergence in South Loyalty Basin that is assumed by some to have opened during this period. If so, this subduction zone did not accommodate convergence between 60 Ma and ~30 Ma despite major absolute plate motion in this window and must thus have terminated at ~60 Ma by slab break-off. If, alternatively, South Loyalty Basin opened between 140 and 120 Ma, as has also been proposed, there is no reason to infer a subduction zone between the Pacific and Australian plates between ~85 and 60 Ma.
2. East-dipping New Caledonia subduction started at ~60 Ma. Subduction was initially very slow but rates increased markedly at ~45 Ma, leading to back-arc extension in North Loyalty Basin. South Loyalty Basin, which had an east–west width of approximately 750 km, was consumed by the New Caledonia subduction zone through to ~30 Ma, consistent with seismic tomographic constraints.
3. Subduction at the Tonga-Kermadec subduction zone started sometime between 45 and 30 Ma. A 30 Ma age of initiation of Tonga-Kermadec subduction is consistent with the results of seismic tomography of the subducted slabs of both the New Caledonia and Tonga-Kermadec subduction zones, but an older age up to 45 Ma cannot be excluded. However, if subduction initiated between 45 and 30 Ma, it was restricted to no more than a few hundred kilometers of slab subduction.
4. When viewed in an absolute plate motion frame, our reconstruction predicts the locations of the New Guinea-Pocklington and New Caledonia subduction zones during their respective 50 Ma and 30 Ma slab detachments that correspond to the present-day location of their associated slabs. Absolute plate motions resulted in 2800 km and 1200 km of northward motion of the New Guinea-Pocklington and New Caledonia sutures relative to the present locations of the Lake Eyre and South Loyalty slabs in the mantle, respectively. This is in agreement with earlier findings by Schellart and coworkers. On the contrary, the Tonga-Kermadec slab, which is still attached to Pacific plate at the surface, does not show any southward offset related to the northward component of absolute plate motion.
5. Since the 30 Ma initiation of subduction, the entire Tonga-Kermadec slab, eventually including its lower-mantle portion, has been dragged laterally through the mantle by some 1,200 km to the north. The effects on slab deformation, mantle anisotropy, seismicity, and focal mechanism, as well as on surface deformation, require further investigation. Particularly, numerical modeling is required to distinguish between the trench-normal and trench-parallel components of slab dragging.

Acknowledgments
D. J. J. v. H. acknowledges ERC Starting grant 306810 (SINK) and NWO Vidi grant 864.11.004. L. M. B. acknowledges NWO grant 824.01.004. P. J. J. K. acknowledges MBIE contract CONT-42907-EMRT-UOW funding. W. S. acknowledges past support of tomography research by the Netherlands Research Centre for Integrated Solid Earth Science (ISES) and support from the Research Council of Norway through its Centres of Excellence funding scheme, project number 223272. All GPlates reconstruction files are available in the supporting information; see also http://www.geologist.nl/reconstructions/. Detailed tomographic images and the UU-P07 tomographic model used for Figures 3, 5, 6, and 7 are available at http://www.atlas-of-the-underworld.org. We acknowledge the comments of the associate editor and two anonymous reviewers, which helped us to improve the manuscript.

References

Amante, C., & Eakins, B. W. (2009). ETOPO1 1 arc-minute global relief model: Procedures, data sources and analysis. In *NOAA technical memorandum NESDIS NGDC-24* (pp. 1–19). National Geophysical Data Center: NOAA. https://doi.org/10.7289/V5C8276M

Amaru, M. L. (2007). Global travel time tomography with 3-D reference models. Ph. D thesis, Utrecht University, the Netherlands.

Auzende, J.-M., Pelletier B., Eissen, J. Ph., (1995). The North Fiji Basin, geology structure and geodynamic evolution. In: Back-arc Basins: *Tectonics and magmatism*, edited by Brian Taylor, Plenum Press, New York. 139–175.

Bache, F., Sutherland, R., Stagpoole, V., Collot, J., & Rouillard, P. (2012). Stratigraphy of the southern Norfolk Ridge and the Reinga Basin: A record of initiation of Tonga-Kermadec-Northland subduction in the southwest Pacific. *Earth and Planetary Science Letters*, *321-322*, 41–53. https://doi.org/10.1016/j.epsl.2011.12.041

Baker, P. E., Coltorti, M., Briqueu, L., Hasenaka, T., Condliffe, E., & Crawford, A. J. (1994). Petrology and composition of the volcanic basement of Bougainville Guyot, Site 831. *Proceeding of the Ocean Drilling Program, Scientific Results*, *134*, 363–373.

Ballance, P. F., & Spörli, K. B. (1979). Northland Allochton. *Journal of the Royal Society of New Zealand*, *9*(2), 259–275. https://doi.org/10.1080/03036758.1979.10419416

Bernardel, G., Carson, L., Meffre, S., Symonds, P., & Mauffret, A. (2002). *Geological and morphological framework of the Norfolk Ridge to Three Kings Ridge region* (p. 76). Canberra: Geoscience Australia.

Bevis, M., Taylor, F. W., Schutz, B. E., Recy, J., Isacks, B. L., Helu, S., et al. (1995). Geodetic observations of very rapid convergence and back-arc extension at the Tonga arc. *Nature*, *374*(6519), 249–251. https://doi.org/10.1038/374249a0

Bijwaard, H., Spakman, W., & Engdahl, E. R. (1998). Closing the gap between regional and global travel time tomography. *Journal of Geophysical Research*, *103*(B12), 30,055–30,078. https://doi.org/10.1029/98JB02467

Bloomer, S. H., Taylor, B., MacLeod, C. J., Stern, R. J., Fryer, P., Hawkins, J. W., & Johnson, L. (1995). Early arc volcanism and the ophiolite problem: A perspective from drilling in the western Pacific. In B. Taylor, & J. Natland (Eds.), *Active Margins and Marginal Basins of the Western Pacific*, *American Geophysical Union Geophysical Monograph* (Vol. 88, pp. 1–30). Washingon, DC: American Geophysical Union. https://doi.org/10.1029/GM088p0001

Boschman, L. M., van Hinsbergen, D. J. J., Torsvik, T. H., Spakman, W., & Pindell, J. L. (2014). Kinematic reconstruction of the Caribbean region since the early Jurassic. *Earth-Science Reviews*, *138*, 102–136. https://doi.org/10.1016/j.earscirev.2014.08.007

Boyden, J., Müller, R. D., Gurnis, M., Torsvik, T. H., Clark, J., Turner, M., et al. (2011). Next-generation plate-tectonic reconstructions using GPlates. In R. Keller, & C. Baru (Eds.), *Geoinformatics: Cyberinfrastructure for the solid earth sciences* (pp. 95–113). Cambridge: Cambridge University Press.

Brothers, R. N., & Delaloye, M. (1982). Obducted ophiolites of North Island: Origin, age, emplacement and tectonic implications for tertiary and quaternary volcanicity. *New Zealand Journal of Geology and Geophysics*, *25*(3), 257–274. https://doi.org/10.1080/00288306.1982.10421491

Cande, S. C., & Stock, J. M. (2004). Cenozoic reconstructions of the Australia-New Zealand-South Pacific sector of Antarctica. In N. F. Exon, J. P. Kennet, & M. J. Malone (Eds.), *The Cenozoic Southern Ocean: Tectonics, sedimentation, and climate change between Australia and Antarctica*, *Geophysical Monograph Series 151* (pp. 5–17). Washington, DC.: American Geophysical Union.

Cande, S. C., Stock, J. M., Müller, R. D., & Ishihara, T. (2000). Cenozoic motion between east and West Antarctica. *Nature*, *404*(6774), 145–150. https://doi.org/10.1038/35004501

Chang, S.-J., Ferreira, A. M. G., & Faccenda, M. (2016). Upper- and mid-mantle interaction between the Samoan plume and the Tonga-Kermadec slabs. *Nature Communications*, *7*, 10799. https://doi.org/10.1038/ncomms10799

Chertova, M. V., Spakman, W., & Steinberger, B. (2018). Mantle flow influence on subduction evolution. *Earth and Planetary Science Letters*, *489*, 258–266. https://doi.org/10.1016/j.epsl.2018.02.038

Chertova, M. V., Spakman, W., Van den Berg, A. P., & Van Hinsbergen, D. J. J. (2014). Absolute plate motions and regional subduction evolution. *Geochemistry, Geophysics, Geosystems*, *15*, 3780–3792. https://doi.org/10.1002/2014GC005494

Cluzel, D., Aitchison, J. C., & Picard, C. (2001). Tectonic accretion and underplating mafic terranes in the late Eocene intraoceanic fore-arc of New Caledonia (Southwest Pacific): Geodynamic implications. *Tectonophysics*, *240*, 23–59.

Cluzel, D., Jourdan, F., Meffre, S., Maurizot, P., & Lesimple, S. (2012). The metamorphic sole of New Caledonia ophiolite: $^{40}Ar/^{39}Ar$, U-Pb, and geochemical evidence for subduction inception at a spreading ridge. *Tectonics*, *31*, TC3016. https://doi.org/10.1029/2011TC003085

Cluzel, D., Maurizot, P., Collot, J.-Y., & Sevin, B. (2012). An outline of the geology of New Caledonia; from Permian-Mesozoic Southeast Gondwanaland active margin to Cenozoic obduction and supergene evolution. *Episodes*, *35*, 72–86.

Cluzel, D., Meffre, S., Maurizot, P., & Crawford, A. J. (2006). Earliest Eocene (53 ma) convergence in the Southwest Pacific: Evidence from pre-obduction dikes in the ophiolite of New Caledonia. *Terra Nova*, *18*(6), 395–402. https://doi.org/10.1111/j.1365-3121.2006.00704.x

Collot, J.-Y., Herzer, R., Lafoy, Y., & Géli, L. (2009). Mesozoic history of the fairway-Aotea Basin: Implications for the early stages of Gondwana fragmentation. *Geochemistry, Geophysics, Geosystems*, *10*, Q12019. https://doi.org/10.1029/2009GC002612

Collot, J.-Y., Lallemand, S., Pelletier, B., Eissen, J.-P., Glaçon, G., Fisher, M. A., et al. (1992). Geology of the d'Entrecasteaux-New Hebrides arc collision zone: Results from a deep submersible survey. *Tectonophysics*, *212*(3-4), 213–241. https://doi.org/10.1016/0040-1951(92)90292-E

Collot, J.-Y., Malahoff, A., Recy, J., Latham, G., & Missegue, F. (1987). Overthrust emplacement of New Caledonia ophiolite: Geophysical evidence. *Tectonics*, *6*(3), 215–232. https://doi.org/10.1029/TC006i003p00215

Conrad, C.P., and Lithgow-Bertelloni, C., 2002. *How slabs drive plate tectonics: Science 298, 207–209*.

Crawford, A. J., Meffre, S., & Symonds, P. A. (2003). 120 to 0 Ma tectonic evolution of the southwest Pacific and analogous geological evolution of the 600 to 220 Ma Tasman Fold Belt System. *Geological Society of Australia Special Publication*, *22*, 377–397.

Croon, M. B., Cande, S. C., & Stock, J. M. (2008). Revised Pacific-Antarctic plate motions and geophysics of the Menard Fracture Zone. *Geochemistry, Geophysics, Geosystems*, *9*, Q07001. https://doi.org/10.1029/2008GC002019

Davey, F. J. (1982). The structure of the South Fiji Basin. *Tectonophysics*, *87*(1-4), 185–241. https://doi.org/10.1016/0040-1951(82)90227-X

Davy, B., Hoernle, K., & Werner, R. (2008). Hikurangi plateau: Crustal structure, rifted for- mation, and Gondwana subduction history. *Geochemistry, Geophysics, Geosystems*, *9*, Q07004. https://doi.org/10.1029/2007GC001855

Doubrovine, P. V., Steinberger, B., & Torsvik, T. H. (2012). Absolute plate motions in a reference frame defined by moving hot spots in the Pacific, Atlantic, and Indian oceans. *Journal of Geophysical Research*, *117*, B09101. https://doi.org/10.1029/2011JB009072

Doubrovine, P. V., & Tarduno, J. A. (2008a). Linking the Late Cretaceous to Paleogene Pacific plate and the Atlantic bordering continents using plate circuits and paleomagnetic data. *Journal of Geophysical Research*, *113*, B07104. https://doi.org/10.1029/2008JB005584

Doubrovine, P. V., & Tarduno, J. A. (2008b). A revised kinematic model for the relative motion between Pacific oceanic plates and North America since the Late Cretaceous. *Journal of Geophysical Research*, *113*, B12101. https://doi.org/10.1029/2008JB005585

Druken, K. A., Kincaid, C., Griffiths, R. W., Stegman, D. R., & Hart, S. R. (2014). Plume-slab interaction: The Samoa-Tonga system. *Physics of the Earth and Planetary Interiors*, *232*, 1–14. https://doi.org/10.1016/j.pepi.2014.03.003

Eissen, J.-P., Crawford, A. J., Cotten, J., Meffre, S., Bellon, H., & Delaune, M. (1998). Geochemistry and tectonic significance of basalts in the Poya Terrane, New Caledonia. *Tectonophysics*, *284*(3-4), 203–219. https://doi.org/10.1016/S0040-1951(97)00183-2

Ewart, A., Brother, R. N., & Mateen, A. (1977). An outline of the geology and geochemistry, and the possible petrogenetic evolution of the volcanic rocks of the Tonga-Kermadec-New Zealand island arc. *Journal of Volcanology and Geothermal Research*, *2*(3), 205–250. https://doi.org/10.1016/0377-0273(77)90001-4

Faccenna, C., Becker, T. W., Lallemand, S., & Steinberger, B. (2012). On the role of slab pull in the Cenozoic motion of the Pacific plate. *Geophysical Research Letters*, *39*, L03305. https://doi.org/10.1029/2011GL050155

Field, B. D., & Uruski, C. I. (1997). Cretaceous-Cenozoic geology and petroleum systems of the East Coast region, New Zealand (Vol. 1). Institute of Geological & Nuclear Sciences.

Fukao, Y., & Obayashi, M. (2013). Subducted slabs stagnant above, penetrating through, and trapped below the 660 km discontinuity. *Journal of Geophysical Research: Solid Earth*, *118*, 5920–5938. https://doi.org/10.1002/2013JB010466

Fukao, Y., Widiyantoro, S., & Obayashi, M. (2001). Stagnant slabs in the upper and lower mantle transition region. *Reviews of Geophysics*, *39*(3), 291–323. https://doi.org/10.1029/1999RG000068

Furlong, K. P., & Govers, R. (1999). Ephemeral crustal thickening at a triple junction: The Mendocino crustal conveyor. *Geology*, *27*(2), 127–130. https://doi.org/10.1130/0091-7613(1999)027<0127:ECTAAT>2.3.CO;2

Furlong, K. P., & Kamp, P. J. J. (2013). Changes in plate boundary kinematics: Punctuated or smoothly varying—Evidence from the Mid-Cenozoic transition from lithospheric extension to shortening in New Zealand. *Tectonophysics*, *608*, 1328–1342. https://doi.org/10.1016/j.tecto.2013.06.008

Gaina, C., Müller, R. D., Royer, J. Y., Stock, J., Hardebeck, J., & Symonds, P. (1998). The tectonic history of the Tasman Sea: A puzzle with 13 pieces. *Journal of Geophysical Research*, *103*, 12,413–12,433.

Gaina, C., Müller, R. D., Royer, J.-Y., & Symonds, P. (1999). Evolution of the Louisiade triple junction. *Journal of Geophysical Research*, *104*(B6), 12,927–12,939. https://doi.org/10.1029/1999JB900038

Giardini, D., & Woodhouse, J. H. (1986). Horizontal shear flow in the mantle beneath the Tonga arc. *Nature*, *319*(6054), 551–555. https://doi.org/10.1038/319551a0

Goes, S., Cammarano, F., & Hansen, U. (2004). Synthetic seismic signature of thermal mantle plumes. *Earth and Planetary Science Letters*, *218*(3-4), 403–419. https://doi.org/10.1016/S0012-821X(03)00680-0

Goes, S., Capitanio, F. A., Morra, G., Seton, M., & Giardini, D. (2011). Signatures of downgoing plate-buoyancy driven subduction in Cenozoic plate motions. *Physics of the Earth and Planetary Interiors*, *184*(1-2), 1–13. https://doi.org/10.1016/j.pepi.2010.10.007

Gorbatov, A., & Kennett, B. L. N. (2003). Joint bulk-sound and shear tomography for Western Pacific subduction zones. *Earth and Planetary Science Letters*, *210*, 527–543.

Granot, R., Cande, S. C., Stock, J. M., & Damaske, D. (2013a). Revised Eocene-Oligocene kinematics for the West Antarctic rift system. *Geophysical Research Letters*, *40*, 279–284. https://doi.org/10.1029/2012GL054181

Granot, R., Cande, S. C., Stock, J. M., & Damaske, D. (2013b). Correction to "Revised Eocene-Oligocene kinematics for the West Antarctic rift system". *Geophysical Research Letters*, *40*, 4625. https://doi.org/10.1002/grl.50727

Hafkenscheid, E., Wortel, M. J. R., & Spakman, W. (2006). Subduction history of the Tethyan region derived from seismic tomography and tectonic reconstructions. *Journal of Geophysical Research*, *111*, B08401. https://doi.org/10.1029/2005JB003791

Hall, R., & Spakman, W. (2002). Subducted slabs beneath the eastern Indonesia-Tonga region: Insights from tomography. *Earth and Planetary Science Letters*, *201*(2), 321–336. https://doi.org/10.1016/S0012-821X(02)00705-7

Hall, R., & Spakman, W. (2004). Mantle structure and tectonic evolution of the region north and east of Australia. *Geological Society of Australia Special Publication*, *22*, 361–381.

Hayes, G. P., Furlong, K. P., & Ammon, C. J. (2009). Intraplate deformation adjacent to the Macquarie ridge south of New Zealand—The tectonic evolution of a complex plate boundary. *Tectonophysics*, *463*(1-4), 1–14. https://doi.org/10.1016/j.tecto.2008.09.024

Herzer, R. H., Barker, D. H. N., Roest, W. R., & Mortimer, N. (2011). Oligocene-Miocene spreading history of the northern South Fiji Basin and implications for the evolution of the New Zealand plate boundary. *Geochemistry, Geophysics, Geosystems*, *12*, Q02004. https://doi.org/10.1029/2010GC003291

Herzer, R. H., Davy, B. W., Mortimer, N., Quilty, P. G., Chaprioniere, G. C. H., Jones, C. M., et al. (2009). Seismic stratigraphy and structure of the Northland Plateau and the development of the Vening Meinesz transform margin, SW Pacific Ocean. *Marine Geophysical Researches*, *30*(1), 21–60. https://doi.org/10.1007/s11001-009-9065-1

Herzer, R. H., & Mascle, J. (1996). Anatomy of a continent-backarc transform—The Vening Meinesz Fracture Zone northwest of New Zealand. *Marine Geophysical Researches*, *18*(2-4), 401–427. https://doi.org/10.1007/BF00286087

Heuret, A., & Lallemand, S. (2005). Plate motions, slab dynamics and back-arc deformations. *Physics of the Earth and Planetary Interiors*, *149*, 31.51.

Hollis, C. J., & Hanson, J. A. (1991). Well-preserved late Paleocene Radiolaria from Tangihua Complex, Camp Bay, eastern Northland. *Tane*, *33*, 65–76.

Ishizuka, O., Tani, K., Reagan, M. K., Kanayama, K., Umino, S., Harigane, Y., et al. (2011). The timescales of subduction initiation and subsequent evolution of an oceanic island arc. *Earth and Planetary Science Letters*, *306*(3-4), 229–240. https://doi.org/10.1016/j.epsl.2011.04.006

Kamp, P. J. J. (1986). The mid-Cenozoic challenger rift system of western New Zealand and its implications for the age of alpine fault inception. *Geological Society of America Bulletin*, *97*(3), 255–281. https://doi.org/10.1130/0016-7606(1986)97<255:TMCRSO>2.0.CO;2

Kamp, P. J. J., van der Wiel, L., Lyon, Z., van de Lagemaat, S. H. A., Boschman, L. M., & van Hinsbergen, D. J. J. (2017). From Global plate kinematics (GPlates) to basin-scale strain expressed in stratigraphy and structure: An application to Taranaki Basin, New Zealand. New Zealand Petroleum Conference 2017, 21–23 March, New Plymouth. Download at: http://www.petroleumconference.nz/past-conferences/2017-presentations/

Keller, W.R., 2004. Cenozoic plate tectonic reconstructions and plate boundary processes in the Southwest Pacific, Ph. D Thesis, California Institute of Technology, Pasadena, CA, 139 pp.

King, P. R. (2000). Tectonic reconstructions of New Zealand: 40 Ma to the present. *New Zealand Journal of Geology and Geophysics*, *43*(4), 611–638. https://doi.org/10.1080/00288306.2000.9514913

Klingelhoefer, F., Lafoy, Y., Collot, J.-Y., Cosquer, E., Géli, L., Nouzé, H., & Vially, R. (2007). Crustal structure of the basin and ridge system west of New Caledonia (southwest Pacific) from wide-angle and reflection seismic data. *Journal of Geophysical Research*, *112*, B11102. https://doi.org/10.1029/2007JB005093

Knesel, K. M., Cohen, B. E., Vasconcelos, P. M., & Thiede, D. S. (2008). Rapid change in drift of the Australian plate records collision with Ontong Java plateau. *Nature*, *454*(7205), 754–757. https://doi.org/10.1038/nature07138

Kroenke, L. W., & Eade, J. V. (1982). Three Kings Ridge: A west-facing arc. *Geo-Marine Letters*, *2*(1-2), 5–10. https://doi.org/10.1007/BF02462793

Lafoy, Y., Géli, L., Klingelhoefer, F., Vially, R., Sichler, B., & Nouzé, H. (2005). Discovery of continental stretching and oceanic spreading in the Tasman Sea. *Eos*, *86*(10), 101–105. https://doi.org/10.1029/2005EO100001

Lafoy, Y., Missegue, F., Cluzel, D., & Le Sauve, R. (1996). The Loyalty-New Hebrides Arc collision: Effects on the Loyalty Ridge and basin system, Southwest Pacific (first results of the ZoNéCo programme). *Marine Geophysical Researches*, *18*(2-4), 337–356. https://doi.org/10.1007/BF00286084

Lagabrielle, Y., Ruellan, E., Tanahashi, M., Bourgois, J., Buffet, G., de Alteriis, G., et al. (1996). Active oceanic spreading in the Northern North Fiji Basin: Results of the NOFI cruise of R/V L'Atalante (Newstarmer Project). *Marine Geophysical Researches*, *18*(2-4), 225–247. https://doi.org/10.1007/BF00286079

Larter, R. D., Cunningham, A. P., Barker, P. F., Gohl, K., & Nitsche, F. O. (2002). Tectonic evolution of the Pacific margin of Antarctica 1. Late Cretaceous tectonic reconstructions. *Journal of Geophysical Research*, *107*(B12), 2345. https://doi.org/10.1029/2000JB000052

Launay, J., Dupont, J., & Lapouille, A. (1982). The Three Kings Ridge and the Norfolk Basin (southwest Pacific): An attempt at structural interpretation. *South Pacific Marine Geological Notes*, *2*, 121–130.

Le Dain, A. Y., Tapponnier, P., & Molnar, P. (1984). Active faulting and tectonics of Burma and surrounding regions. *Journal of Geophysical Research*, *89*(B1), 453–472. https://doi.org/10.1029/JB089iB01p00453

Maillet, P., Monzier, M., Selo, M., & Storzer, D. (1983). The D'Entrecasteaux Zone (Southwest Pacific). A petrological and geochronological reappraisal. *Marine Geology*, *53*(3), 179–197. https://doi.org/10.1016/0025-3227(83)90073-7

Malahoff, A., Feden, R. H., & Fleming, H. S. (1982). Magnetic anomalies and tectonic fabric of marginal basins north of New Zealand. *Journal of Geophysical Research*, *87*(B5), 4109–4125. https://doi.org/10.1029/JB087iB05p04109

Malahoff, A., Kroenke, L. W., Cherkis, N., & Brozena, J. (1994). Magnetic and tectonic fabric in the North Fiji Basin and Lau Basin. In L. W. Kroenke, & J. V. Eade (Eds.), *Basin formation, ridge crest processes and metalogenesis in the North Fiji Basin*, *Circum Pacific Council for Energy and Mineral Resources, Earth Science Series* (Vol. 15, pp. 49–63). Berlin, Heidelberg: Springer. https://doi.org/10.1007/978-3-642-85043-1_6

Malpas, J., Spörli, K. B., Black, P. M., & Smith, I. E. M. (1992). Northland ophiolite, New Zealand, and implications for plate-tectonic evolution of the Southwest Pacific. *Geology*, *20*(2), 149–152. https://doi.org/10.1130/0091-7613(1992)020<0149:NONZAI>2.3.CO;2

Marchesi, C., Garrido, C. J., Godard, M., Belley, F., & Ferre, E. (2009). Migration and accumulation of ultra-depleted subduction related melts in the Massif du Sud ophiolite (New Caledonia). *Chemical Geology*, *266*, 180–195.

Matthews, K. J., Hale, A. J., Gurnis, M., Müller, R. D., & DiCaprio, L. (2011). Dynamic subsidence of Eastern Australia during the Cretaceous. *Gondwana Research*, *19*(2), 372–383. https://doi.org/10.1016/j.gr.2010.06.006

Matthews, K. J., Seton, M., & Müller, R. D. (2012). A global-scale plate reorganization event at 105–100 Ma. *Earth and Planetary Science Letters*, *355–356*, 283–298.

Matthews, K. J., Williams, S. E., Whittaker, J. M., Müller, R. D., Seton, M., & Clarke, G. L. (2015). Geologic and kinematic constraints on Late Cretaceous to mid Eocene plate boundaries in the southwest Pacific. *Earth-Science Reviews*, *140*, 72–107. https://doi.org/10.1016/j.earscirev.2014.10.008

Mazengarb, C., & Speden, I. G. (2000). Geology of the Raukumara area. Institute of Geological & Nuclear Sciences 1:250 000 Geological Map 6.1 Sheet + 60 p. Lower Hutt, New Zealand. Institute of Geological & Nuclear Sciences Limited.

Meffre, S., Symonds, P., Bernardel, G., Carson, L., & Mauffret, A. (2001). Basalts, sedimentary rocks and peridotites of the Three Kings Ridge: Implications for the initiation of convergence along the Tonga-Kermadec Arc, in paper presented at Fifth Australian Marine Geoscience Conference, Consortium for Ocean Geosciences of Australian Universities, Hobart, Australia.

Mortimer, N., Herzer, R. H., Gans, P. B., Laporte-Magoni, C., Calvert, A. T., & Bosch, D. (2007). Oligocene–Miocene tectonic evolution of the South Fiji Basin and Northland Plateau, SW Pacific Ocean: Evidence from petrology and dating of dredged rocks. *Marine Geology*, *237*(1-2), 1–24. https://doi.org/10.1016/j.margeo.2006.10.033

Mortimer, N., Herzer, R. H., Gans, P. B., Parkinson, D. L., & Seward, D. (1998). Basement geology from Three Kings Ridge to West Norfolk Ridge, Southwest Pacific Ocean: Evidence from petrology, geochemistry and isotopic dating of dredge samples. *Marine Geology*, *148*(3-4), 135–162. https://doi.org/10.1016/S0025-3227(98)00007-3

Müller, R. D., Seton, M. S., Zahirovic, S., Williamd, S. E., Matthews, K. J., Wright, N. M., et al. (2016). Ocean basin evolution and global-scale plate reorganization events since Pangea breakup. *Annual Review of Earth and Planetary Science Letters*, *44*(1), 107–138. https://doi.org/10.1146/annurev-earth-060115-012211

Nicholson, K. N., Black, P. M., & Picard, C. (2000). Geochemistry and tectonic significance of the Tangihua Ophiolite Complex, New Zealand. *Tectonophysics*, *321*(1), 1–15. https://doi.org/10.1016/S0040-1951(00)00081-0

Nicholson, K. N., Black, P. M., Picard, C., Cooper, P., Hall, C. M., & Itaya, T. (2007). Alteration, age, and emplacement of the Tangihua Complex Ophiolite, New Zealand. *New Zealand Journal of Geology and Geophysics*, *50*(2), 151–164. https://doi.org/10.1080/00288300709509827

Nicholson, K. N., Picard, C., & Black, P. M. (2000). A comparative study of Late Cretaceous ophiolitic basalts from New Zealand and New Caledonia: Implications for the tectonic evolution of the SW Pacific. *Tectonophysics*, *327*(3-4), 157–171. https://doi.org/10.1016/S0040-1951(00)00167-0

Obayashi, M., Yoshimitsu, J., Nolet, G., Fukao, Y., Shiobara, H., Sugioka, H., et al. (2013). Finite frequency whole mantle P wave tomography: Improvement of subducted slab images. *Geophysical Research Letters*, *40*, 5652–5657. https://doi.org/10.1002/2013GL057401

Ogg, J. G. (2012). Chapter 5—Geomagnetic polarity time scale. In F. M. Gradstein, J. G. Ogg, M. Schmitz, & G. Ogg (Eds.), *The geologic time scale* (pp. 85–113). Boston: Elsevier. https://doi.org/10.1016/B978-0-444-59425-9.00005-6

O'Neill, C. J., Müller, R. D., & Steinberger, B. (2005). On the uncertainties in hotspot reconstructions and the significance of moving hotspot reference frames. *Geochemistry, Geophysics, Geosystems*, *6*, Q04003. https://doi.org/10.1029/2004GC000784

Packham, G. H., & Terrill, A. (1975). Submarine geology of the South Fiji basin. *Initial Reports of the Deep Sea Drilling Project*, *30*, 617–645.

Paquette, J.-L., & Cluzel, D. (2007). U-Pb zircon dating of post-obduction volcanic-arc granitoids and a granulite-facies xenolith from New Caledonia. Inference on Southwest Pacific geodynamic models. *International Journal of Earth Sciences*, *96*, 613–622.

Parson, L. M., & Wright, I. C. (1996). The Lau-Havre-Taupo back-arc basin: A southward-propagating, multi-stage evolution from rifting to spreading. *Tectonophysics*, *263*(1-4), 1–22. https://doi.org/10.1016/S0040-1951(96)00029-7

Petterson, M., Neal, C., Mahoney, J., Kroenke, L., Saunders, A., Babbs, T., et al. (1997). Structure and deformation of north and central Malaita, Solomon Islands: Tectonic implications for the Ontong Java Plateau-Solomon arc collision, and for the fate of oceanic plateaus. *Tectonophysics*, *283*(1-4), 1–33. https://doi.org/10.1016/S0040-1951(97)00206-0

Philippon, M., & Corti, G. (2016). Obliquity along plate boundaries. *Tectonophysics*, *693*, 171–182. https://doi.org/10.1016/j.tecto.2016.05.033

Pikser, J. E., Forsyth, D. W., & Hirth, G. (2012). Along-strike translation of a fossil slab. *Earth and Planetary Science Letters*, *331-332*, 315–321. https://doi.org/10.1016/j.epsl.2012.03.027

Prinzhofer, A. (1981). Structure et pétrologie d'un cortège ophiolitique: Le massif du sud (Nouvelle Calédonie), Ph. D Thesis. École Nationale Supérieure des Mines de Paris, France.

Quarles van Ufford, A., & Cloos, M. (2005). Cenozoic tectonics of New Guinea. *AAPG Bulletin*, *89*(1), 119–140. https://doi.org/10.1306/08300403073

Quesnel, B., Gautier, P., Cathelineau, M., Boulvais, P., Couteau, C., & Drouillet, M. (2016). The internal deformation of the Peridotite Nappe of New Caledonia: A structural study of serpentine-bearing faults and shear zones in the Koniambo Massif. *Journal of Structural Geology*, *85*, 51–67.

Rouillard, P., Collot, J., Sutherland, R., Bache, F., Patriat, M., Etienne, S., & Maurizot, P. (2017). Seismic stratigraphy and paleogeographic evolution of Fairway Basin, Northern Zealandia, Southwest Pacific: From Cretaceous Gondwana breakup to Cenozoic Tonga-Kermadec subduction. *Basin Research*, *29*, 189–212. https://doi.org/10.1111/bre.12144

Ruellan, E., Delteil, J., Wright, I., & Matsumoto, T. (2003). From rifting to active spreading in the Lau Basin-Havre Trough backarc system (SW Pacific): Locking/unlocking induced by seamount chain subduction. *Geochemistry, Geophysics, Geosystems*, *4*(5), 8909. https://doi.org/10.1029/2001GC000261

Schellart, W. P. (2005). Influence of the subducting plate velocity on the geometry of the slab and migration of the subduction hinge. *Earth and Planetary Science Letters*, *231*(3-4), 197–219. https://doi.org/10.1016/j.epsl.2004.12.019

Schellart, W. P. (2007). North-eastward subduction followed by slab detachment to explain ophiolite obduction and Early Miocene volcanism in Northland, New Zealand. *Terra Nova*, *19*(3), 211–218. https://doi.org/10.1111/j.1365-3121.2007.00736.x

Schellart, W. P., Kennet, B. L. N., Spakman, W., & Amaru, M. (2009). Plate reconstructions and tomography reveal a fossil lower mantle slab below the Tasman Sea. *Earth and Planetary Science Letters*, *278*(3-4), 143–151. https://doi.org/10.1016/j.epsl.2008.11.004

Schellart, W. P., Lister, G. S., & Toy, V. G. (2006). A Late Cretaceous and Cenozoic reconstruction of the Southwest Pacific region: Tectonics controlled by subduction and slab rollback processes. *Earth-Science Reviews*, *76*(3-4), 191–233. https://doi.org/10.1016/j.earscirev.2006.01.002

Schellart, W. P., & Spakman, W. (2012). Mantle constraints on the plate tectonic evolution of the Tonga–Kermadec–Hikurangi subduction zone and the South Fiji Basin region. *Australian Journal of Earth Sciences*, *59*(6), 933–952. https://doi.org/10.1080/08120099.2012.679692

Schellart, W. P., & Spakman, W. (2015). Australian plate motion and topography linked to fossil New Guinea slab below Lake Eyre. *Earth and Planetary Science Letters*, *421*, 107–116. https://doi.org/10.1016/j.epsl.2015.03.036

Schellart, W. P., Stegman, D. R., & Freeman, J. (2008). Global trench migration velocities and slab migration induced upper mantle volume fluxes: Constraints to find an Earth reference frame based on minimizing viscous dissipation. *Earth-Science Reviews*, *88*, 118–144.

Sdrolias, M., Müller, R. D., & Gaina, C. (2001). Plate tectonic evolution of eastern Australian marginal ocean basins. In K. C. Hill & T. Bernecker (Eds.), *Eastern Australian Basins Symposium* (pp. 227–237). Melbourne: Petroleum Exploration Society of Australia Special Publication.

Sdrolias, M., Müller, R. D., & Gaina, C. (2003). Tectonic evolution of the southwest Pacific using constraints from backarc basins. *Geological Society of America Special Papers*, *372*, 343–359.

Sdrolias, M., Müller, R. D., Mauffret, A., & Bernardel, G. (2004). Enigmatic formation of the Norfolk Basin, SW Pacific: A plume influence on back-arc extension. *Geochemistry, Geophysics, Geosystems*, *5*, Q06005. https://doi.org/10.1029/2003GC000643

Sdrolias, M., & Müller, R. D. (2006). Controls on back-arc basin formation. *Geochemistry, Geophysics, Geosystems*, *7*, Q04016. https://doi.org/10.1029/2005GC001090

Seton, M., Müller, R. D., Zahirovic, S., Gaina, C., Torsvik, T., Shephard, G., et al. (2012). Global continental and ocean basin reconstructions since 200 Ma. *Earth-Science Reviews*, *113*(3-4), 212–270. https://doi.org/10.1016/j.earscirev.2012.03.002

Sevin, B., Cluzel, D., Maurizot, P., Quesnel, F., Ricordel-Prognon, C., Chapronniere, G., et al. (2014). A drastic Lower Miocene regolith evolution triggered by post obduction slab break-off and uplift in New Caledonia. *Tectonics*, *33*, 1787–1801. https://doi.org/10.1002/2014TC003588

Spakman, W., Chertova, M. V., Van den Berg, A., & Van Hinsbergen, D. J. J. (2018). Puzzling features of the western Mediterranean tectonics explained by slab dragging. *Nature Geoscience*, *11*(3), 211–216. https://doi.org/10.1038/s41561-018-0066-z

Spakman, W., & Hall, R. (2010). Surface deformation and slab-mantle interaction during Banda arc subduction rollback. *Nature Geoscience*, *3*(8), 562–566. https://doi.org/10.1038/ngeo917

Spiegel, C., Lindow, J., Kamp, P. J. J., Meisel, O., Musaka, S., Lisker, F., et al. (2016). Tectonomorphic evolution of Marie Byrd Land—Implications for Cenozoic rifting activity and onset of West Antarctic glaciation. *Global and Planetary Change*, *145*, 98–115. https://doi.org/10.1016/j.gloplacha.2016.08.013

Steinberger, B., Sutherland, R., & O'Connell, R. J. (2004). Prediction of the Emperor-Hawaii seamount locations from a revised model of global plate motion and mantle flow. *Nature*, *430*(6996), 167–173. https://doi.org/10.1038/nature02660

Stoneley, R. (1968). A lower tertiary decollement on the East Coast, North Island, New Zealand. *New Zealand Journal of Geology and Geophysics*, *11*(1), 128–156. https://doi.org/10.1080/00288306.1968.10423680

Sutherland, R. (1999). Basement geology and tectonic development of the greater New Zealand region: An interpretation from regional magnetic data. *Tectonophysics*, *308*(3), 341–362. https://doi.org/10.1016/S0040-1951(99)00108-0

Sutherland, R., Collot, J., Bache, F., Henrys, S., Barker, D., Browne, G. H., et al. (2017). Widespread compression associated with Eocene Tonga-Kermadec subduction initiation. *Geology*, *45*(4), 355–358. https://doi.org/10.1130/G38617.1

Sutherland, R., & Hollis, C. (2001). Cretaceous demise of the Moa Plate and strike-slip motion at the Gondwana margin. *Geology*, *29*(3), 279–282. https://doi.org/10.1130/0091-7613(2001)029<0279:CDOTMP>2.0.CO;2

Taylor, G. K., Gascoyne, J., & Colley, H. (2000). Rapid rotation of Fiji: Paleomagnetic evidence and tectonic implications. *Journal of Geophysical Research*, *105*(B3), 5771–5781. https://doi.org/10.1029/1999JB900305

Tikku, A. A., & Cande, S. C. (1999). The oldest magnetic anomalies in the Australian-Antarctic Basin: Are they isochrons? *Journal of Geophysical Research*, *104*(B1), 661–677. https://doi.org/10.1029/1998JB900034

Tikku, A. A., & Cande, S. C. (2000). On the fit of Broken Ridge and Kerguelen Plateau. *Earth and Planetary Science Letters*, *180*(1-2), 117–132. https://doi.org/10.1016/S0012-821X(00)00157-6

Torsvik, T. H., Müller, R. D., Van der Voo, R., Steinberger, B., & Gaina, C. (2008). Global plate motion frames: Toward a unified model. *Reviews of Geophysics*, *46*, RG3004. https://doi.org/10.1029/2007RG000227

Turcotte, D. L., & Schubert, G. (2002). *Geodynamics* (456 pp.). Cambridge, UK: Cambridge University Press. https://doi.org/10.1017/CBO9780511807442

Ulrich, M., Picard, C., Guillot, S., Chauvel, C., Cluzel, D., & Meffre, S. (2010). Multiple melting stages and refertilization as indicators for ridge to subduction formation: The New Caledonia ophiolite. *Lithos*, *115*(1-4), 223–236. https://doi.org/10.1016/j.lithos.2009.12.011

Van de Beuque, S., Stagg, H. M. J., Sayers, J., Willcox, J. B., & Symonds, P. A. (2003). Geological framework of the Northern Lord Howe Rise and adjacent areas. *Geoscience Australia Record*, *2003*, 1–116.

Van der Hilst, R. D. (1995). Complex morphology of subducted lithosphere in the mantle beneath the Tonga trench. *Nature*, *374*(6518), 154–157. https://doi.org/10.1038/374154a0

Van der Meer, D. G., van Hinsbergen, D. J. J., & Spakman, W. (2018). The Atlas of the Underworld: A catalogue of slab remnants in the mantle imaged by seismic tomography, and their geological interpretation. *Tectonophysics*, *723*, 309–448.

Van Hinsbergen, D. J. J., Peters, K., Maffione, M., Spakman, W., Guilmette, C., Thieulot, C., et al. (2015). Dynamics of intraoceanic subduction initiation: 2. Suprasubduction zone ophiolite formation and metamorphic sole exhumation in context of absolute plate motions. *Geochemistry, Geophysics, Geosystems*, *16*, 1771–1785. https://doi.org/10.1002/2015GC005745

Wang, Y., Forsyth, D. W., Rau, C. J., Carriero, N., Schmandt, B., Gaherty, J. B., & Savage, B. (2013). Fossil slabs attached to unsubducted fragments of the Farallon plate. *Proceedings of the National Academy of Sciences*, *110*, 5342–5346.

Watts, A. B., Weissel, J. K., & Larson, L. R. (1977). Sea-floor spreading in marginal basins of the western Pacific. *Tectonophysics*, *37*(1-3), 167–181. https://doi.org/10.1016/0040-1951(77)90046-4

Weissel, J. K., Watts, A. B., & Lapouille, A. (1982). Evidence for Late Paleocene to Late Eocene seafloor spreading in the Southern New Hebrides Basin. *Tectonophysics*, *87*(1-4), 243–251. https://doi.org/10.1016/0040-1951(82)90228-1

Whattam, S. A., Malpas, J., Ali, J. R., Lo, C.-H., & Smith, I. E. M. (2005). Formation and emplacement of the Northland ophiolite, northern New Zealand: SW Pacific tectonic implications. *Journal of the Geological Society, London*, *162*(2), 225–241. https://doi.org/10.1144/0016-764903-167

Whattam, S. A., Malpas, J., Ali, J. R., & Smith, I. E. M. (2008). New SW Pacific tectonic model: Cyclical intraoceanic magmatic arc construction and near-coeval emplacement along the Australia-Pacific margin in the Cenozoic. *Geochemistry, Geophysics, Geosystems*, *9*, Q03021. https://doi.org/10.1029/2007GC001710

Whattam, S. A., Malpas, J., Ali, J. R., Smith, I. E. M., & Lo, C.-H. (2004). Origin of the Northland Ophiolite, northern New Zealand: Discussion of new data and reassessment of the model. *New Zealand Journal of Geology and Geophysics*, *47*(3), 383–389. https://doi.org/10.1080/00288306.2004.9515064

Whattam, S. A., Malpas, J., Smith, I. E. M., & Ali, J. R. (2006). Link between SSZ ophiolite formation, emplacement and arc inception, Northland, New Zealand: U-Pb SHRIMP constraints; Cenozoic SW Pacific tectonic implications. *Earth and Planetary Science Letters*, *250*(3-4), 606–632. https://doi.org/10.1016/j.epsl.2006.07.047

Whittaker, J. M., Müller, R. D., Leitchenkov, G., Stagg, H., Sdrolias, M., Gaina, C., & Goncharov, A. (2007). Major Australian-Antarctic plate reorganization at Hawaiian-Emperor Bend time. *Science*, *318*(5847), 83–86. https://doi.org/10.1126/science.1143769

Whittaker, J. M., Williams, S. E., & Müller, R. D. (2013). Revised tectonic evolution of the Eastern Indian Ocean. *Geochemistry, Geophysics, Geosystems*, *14*, 1891–1909. https://doi.org/10.1002/ggge.20120

Williams, S. E., Whittaker, J. M., & Müller, R. D. (2011). Full-fit, palinspastic reconstruction of the conjugate Australian-Antarctic margins. *Tectonics*, *30*, TC6012. https://doi.org/10.1029/2011TC002912

Wood, R., & Woodward, D. (2002). Sediment thickness and crustal structure of offshore western New Zealand from 3D gravity modelling. *New Zealand Journal of Geology and Geophysics*, *45*(2), 243–255. https://doi.org/10.1080/00288306.2002.9514971

Worthington, T. J., Hekinian, R., Stoffers, P., Kuhn, T., & Hauff, F. (2006). Osbourn Trough: Structure, geochemistry and implications of a mid-Cretaceous paleospreading ridge in the South Pacific. *Earth and Planetary Science Letters*, *245*(3-4), 685–701. https://doi.org/10.1016/j.epsl.2006.03.018

Wright, I. C. (1993). Pre-spread rifting and heterogeneous volcanism in the southern Havre Trough back-arc basin. *Marine Geology*, *113*(3-4), 179–200. https://doi.org/10.1016/0025-3227(93)90017-P

Wright, N. M., Müller, R. D., Seton, M., & Williams, S. E. (2015). Revision of Paleogene plate motion in the Pacific and implications for the Hawaiian-Emperor bend. *Geology*, *43*(5), 455–458. https://doi.org/10.1130/G36303.1

Wright, N. M., Seton, M., Williams, S. E., & Müller, R. D. (2016). The Late Cretaceous to recent tectonic history of the Pacific Ocean basin. *Earth-Science Reviews*, *154*, 138–173. https://doi.org/10.1016/j.earscirev.2015.11.015

Wu, J., Suppe, J., Lu, R., & Kanda, R. (2016). Philippine Sea and East Asian plate tectonics since 52 Ma constrained by new subducted slab reconstruction methods. *Journal of Geophysical Research: Solid Earth*, *121*, 4670–4741. https://doi.org/10.1002/2016JB012923

Wysoczanski, R. J., Todd, E., Wright, I. C., Leybourne, M. I., Hergt, J. M., Adam, C., & Mackay, K. (2010). Backarc rifting, constructional volcanism and nascent disorganised spreading in the southern Havre Trough backarc rifts (SW Pacific). *Journal of Volcanology and Geothermal Research*, *190*(1-2), 39–57. https://doi.org/10.1016/j.jvolgeores.2009.04.004

Yan, C. Y., & Kroenke, L. W. (1993). A plate tectonic reconstruction of the Southwest Pacific, 0-100 Ma. *Oceanic Drilling Program, Scientific Results*, *130*, 697–709.